Hollow CuO microparticles for the efficient degradation of model pollutant dyes

by

SAGYNTAY SARSENOV

2022

Thesis submitted to the School of Sciences and Humanities of Nazarbayev University in Partial Fulfillment of the Requirements for the Degree of

Master of Science in Chemistry

Nazarbayev University

17th July, 2022

ACKNOWLEDGEMENTS

I would like to express my warm appreciation and sincerest gratitude to Dr. Timur Atabaev, my advisor, who provided encouregment, support, and opportunity to work on my thesis and finish it, especially for his invaluable guidance and suggestions to improve my thesis. I am very thankful for being a member of his Advanced Nanomaterials Lab.

In addition, I would like to thank Dr. Anara Molkenova for explaining concepts to me in a clear and concise way, helping me structure my thesis and her overall good humor. It has truly been a pleasure working with her. Also, I would like to thank all professors whose classes I have taken during the Master's program.

Finally, I would like to extend my thanks to my family for their support, especially many thanks to my spouse Amina and daughter Alaina for being with me and motivation to accomplish my Master's degree.

ORIGINALITY STATEMENT

I, Sagyntay Sarsenov, hereby declare that this submission is my own work and to the best of my knowledge it contains no materials previously published or written by another person, or substantial proportions of material which have been accepted for the award of any other degree or diploma at Nazarbayev University or any other educational institution, except where due acknowledgement is made in the thesis.

Any contribution made to the research by others, with whom I have worked at NU or elsewhere is explicitly acknowledged in the thesis.

I also declare that the intellectual content of this thesis is the product of my own work, except to the extent that assistance from others in the project's design and conception or in style, presentation, and linguistic expression is acknowledged.

Signed on 17/07/2022

_____

ABSTRACT

Copper(II) oxide (CuO) is a widely used material in different industries due to its low price, readily availability, long-term photostability, and ability to oxidize different types of organics compounds. However, bare CuO has photocatalytic activity restriction because it cannot generate enough hydroxyl radicals to degrade organic pollutants itself. In this study, H_2O_2-assisted hollow CuO microspheres were utilized for solar light-activated degradation of model pollutant dyes such as rhodamine B and methylene blue. Morphological analysis revealed that synthesized hollow CuO microspheres with a diameter of ~11–20 μm were composed of small crystal strips pointed towards the center of the microsphere. Nitrogen adsorption-desorption experiments revealed that prepared hollow CuO microspheres have a specific surface area of ~12.184 m^2/g. In particular, synthesized CuO microspheres substantially accelerate the degradation rate of aqueous rhodamine B and methylene blue solutions as compared to commercially available CuO nanoparticles and some other CuO structures reported up to date. The recyclability test revealed that hollow CuO microspheres can be re-used several times without losing the photocatalytic activity.

TABLE OF CONTENTS

TABLE OF CONTENTS……..……...4

LIST OF FIGURES…….6

LIST OF TABLES……8

LIST OF ABBREVIATIONS……..9

1. INTRODUCTION……..10

1.1 Background information…..……...10

1.2 Information about dyes….……...……...11

1.3 Wastewater treatment methods…..……12

1.4 Photototcatalysis mechanism...……...…….14

1.5 Influencing factors……...……...…….15

1.5.1 Band gap……...……16

1.5.2 Band gap engineering...……...……17

1.5.3 Charge mobility and material stability……...……...……18

1.5.4 Catalyst loading……..……...……19

1.5.5 Dye loading……...……20

1.5.6 Dye adsorption……..……...……20

1.5.7 Light intensity……...……...……21

1.5.8 Temperature……...……...……21

1.5.9 pH of solution……...……22

1.5.10 Additives…...……...……23

1.6 Overview of photocatalysts……....……...…...24

1.7 CuO photocatalyst…...……....……...……25

1.8 Literature review……....……...……28

1.9 Aims of the present study……....……...……..29

2. METHODOLOGY…….31

2.1 Materials……...……..31

2.2 Synthesis……..……..31

2.2.1 CuO photocatalyst……...……...31

2.2.2 Dye solutions ……..……31

2.3 Sample Characterization……...……...31

2.4 Photocatalytic activity test……..……..32

3. RESULTS & DISCUSSION……..33

3.1 Morphological analysis……...……..33

3.2 Compositional analysis……...……..35

3.3 Optical analysis……...……..36

3.4 BET and BJH analysis……...……...37

3.5 Photocatalytic activity analysis……...…….37

3.5.1 Comparison with commercial CuO……...…….40

3.5.2 One-pot recyclability tests……...……41

3.5.3 Tests in acidic conditions……...……..42

3.5.4 Tests in basic conditions……...……44

4. CONCLUSION……...46

5. LIMITATIONS & FURTHER STUDIES……....47

6. REFERENCES……...48

LIST OF FIGURES

Figure 1. Photocatalysis mechanism. Reprinted from [35]……...……..14

Figure 2. Band gap and band edge positions of semiconductors. Reprinted from [45]……..17

Figure 3. CuO molecular structure. Reprinted from [101]……..……25

Figure 4. Various CuO shapes. Reprinted from [114]…….……26

Figure 5. Low-magnification SEM images of hollow CuO microspheres……...……33

Figure 6. Close up SEM images of hollow CuO microspheres……...33

Figure 7. TEM image of prepared CuO microspheres…….……34

Figure 8. SEM images of commercial CuO……...……..34

Figure 9. Chemical analysis by EDX…….....35

Figure 10. XRD analysis of CuO..……...35

Figure 11. (left) UV-Vis analysis of CuO and (right) indirect bandgap calculation……36

Figure 12. (left) Nitrogen adsorption-desorption isotherms and (right) BJH pore size distribution……37

Figure 13. Absorbance intensity of (left) RB and (right) MB with CuO + H_2O_2…….....37

Figure 14. RB degradation with (red) CuO + H_2O_2; (black) H_2O_2……..……38

Figure 15. MB degradation with (blue) CuO + H_2O_2 and (black) H_2O_2……..……38

Figure 16. CuO + H_2O_2 degradation kinetics for (blue) MB and (red) RB……..……39

Figure 17. Absorbance intensity of (left) RB and (right) MB with commercial CuO + H_2O_2...……..40

Figure 18. RB degradation with (red) commercial CuO + H_2O_2 and (black) prepared CuO + H_2O_2……..40

Figure 19. MB degradation with (blue) commercial CuO + H_2O_2 and (black) prepared CuO + H_2O_2……41

Figure 20. Absorbance intensity of (left) RB and (right) MB with recycled CuO + H_2O_2……..41

Figure 21. Recyclability tests of (red) RB and (blue) MB……...42

Figure 22. Absorbance intensity of (left) RB and (right) MB with acidic CuO + H_2O_2……..43

Figure 23. Degradation of (red) RB and (blue) MB with CuO + H_2O_2 in acidic conditions…..…….43

Figure 24. Absorbance intensity of (left) RB and (right) MB with basic CuO + H_2O_2……...44

Figure 25. Degradation of (red) RB and (blue) MB with CuO + H_2O_2 in basic conditions……45

LIST OF TABLES

Table 1. The efficiency of some CuO-based structures for rhodamine B degradation……28

Table 2. The efficiency of some CuO-based structures for methylene blue degradation……....28

LIST OF ABBREVIATIONS

AOP	Advanced oxidative process
BJH	Barret-Joyner-Halenda
BET	Brunauer-Emmet-Teller
CB	Conduction band
COD	Chemical oxygen demand
EDX	Energy dispersive X-ray
MB	Methylene blue
NIR	Near-infrared
RB	Rhodamine B
ROS	Reactive oxygen species
SEM	Scanning Electron Microscopy
TEM	Transmission Electron Microscopy
UV	Ultraviolet
VB	Valence band
XRD	X-ray diffraction
XPS	X-ray photoelectron spectroscopy

1. INTRODUCTION

1.1 Background information

Water is essential for all living things on the planet. It has no substitutes, so its value cannot be evaluated. Currently, too much pressure has been put on water resources by the growing population and increasing standards of life. Considering that only a tiny amount of total water resources is drinkable, saving as much water as we can is a primary need for humanity. However, the limited amount of freshwater has been turned into wastewater by water contaminants and pollutants produced mainly by industrial processes. In recent years, due to rapid industrial sector growth, organic pollutants such as dyes, pharmaceuticals, etc., have seriously contaminated the environment, especially water bodies. The pollution level is increasing annually at an alarming rate. Some of these pollutants can be carcinogenic or toxic to living organisms, including humans [1-3].

In addition, there is a growth in demand for water in the agricultural, domestic and industrial sectors, which produce large amounts of contaminated effluents. The general classes of compounds that occur in polluted water are dyes, solvents, dibenzofurans, dioxins, pesticides, chlorophenols, asbestos, polychlorinated biphenyls, arsenic, and heavy metals [4,5]. Among these given pollutants, dyes are a serious contributor.

An important kind of organic pollutant is organic dyes. They are used in printing, photographic and textile industries. The issue is that a huge fraction of them is lost during the dyeing process, and then go to water streams with effluents. Generally, even low amounts of dyes in wastewater can negatively affect the nature of water [6-8]. Currently, it is estimated that approximately 0.7 million tons of over 10000 types of organic dyes are used annually [9]. Moreover, approximately 20% of the used dyes are released as textile waste [10]. Despite the fact that it is the responsibility of dye manufacturers to develop an eco-friendly dyeing process, the presence of organic dyes in a discharge cannot be fully excluded. Therefore, an increasing number of effluents are discharged to water resources from industries, wastewater treatment becomes a significant challenge.

Mainly, dyes are stable and it is often a hard task to decompose them in water, as they have complex molecular structures which cause them to be more resistant to biodegradation and stable toward light [11,12]. Dye contaminated wastewater is considered to have an elevated chemical oxygen demand (COD) due to the presence of organic compounds, a high inorganic dissolved substance content, low degradability by biological reagents, and inconsistent pH. During the reduction process of dyes and their intermediates, the production of strong mutagenic or carcinogenic substances can occur, which has an adverse effect on aquatic life and microorganisms [13]. Human intake of water polluted with these compounds can induce a plenty of adverse health effects, such as wide‑ranging immune suppression, central nervous system disorders, breathing problems, allergic reactions, behavioral problems, tissue necrosis, and infections of the eyes and skin [14].

1.2 Information about dyes

Molecules of dyes are commonly composed of two main components: chromophores and auxochromes. The chromophore part absorbs light with a certain wavelength to produce the color. Auxochrome part complements the chromophore and enhances dye color by facilitating the molecule to dissolve in water. Dyes demonstrate large structural diversity and are classified by their chemical constitution and the fabric type to which they are applied. Dyes can also be categorized on the basis of their solubility in different solvents. These include acidic, basic, mordant, reactive, direct and metal complex-based dyes. Insoluble dyes include different types of sulfur, vat, disperse and azoic dyes. Additionally, dyes can also be classified based on the presence and type of anthraquinone and/or azo unit [15]. It was found that only 47% of dyes are biodegrading naturally over time, while others can have long-term side effects on the environment and living organisms [16].

Various types of dyes are used as model organic molecules to study the performance of water treatment methods because it is relatively easy to measure and analyze their concentration by spectroscopic techniques.

1.3 Wastewater treatment methods

Clean water sources have attracted enormous attention because of the critical demand for it as a consequence of the rapid urbanization and industrialization, as well as the huge population increase. As the staggering discharge of pollutants and contaminants into the water cycle is getting higher, the difference in clean water availability and demand is expected to worsen. Concerning the environment, recycling and reuse of effluents is required to increase the limited fresh water supply and to discover more possible water resources in the long run [17]. During the past few decades, different kinds of practical methods have been studied to develop wastewater treatment technologies of great vitality.

There has been growing interest in organic pollutant removal from wastewater. Solids - such as fabrics, food, and plastics can be relatively easily filtered, but the problem arises with dye molecules. They cannot be effectively removed using traditional treatment methods like physical, chemical and biological techniques. Despite their cons, these methods are widely used in textile industries. Generally, physical methods such as adsorption, filtration, coagulation and membrane separation are effective, but they are too expensive due to the need for further treatment of coagulated and solid wastes [18-20]. Biological methods are not suitable for synthetic dyes because they are usually stable to aerobic biodegradation [18,21,22]. Conventionally, biological treatments of wastewater were designed to efficiently remove mixed types of pollutants in the short term; however, these treatment methods also usually lead to the creation of secondary pollution [23], some of which can be health-threatening bacteria and soluble refractory organic compounds that are difficult to eliminate [24].

Low efficiency, large amount of reagents needed, incomplete mineralization and carcinogenic, and toxic byproducts, are all disadvantages of chemical methods that include precipitation, ozonation and chlorination [21,22]. An alternative treatment method used to degrade dyes is oxidation [25]. The oxidation process utilizes reagents such as molecular oxygen (O_2), ozone (O_3), or hydrogen peroxide (H_2O_2). However, a restriction of this process is the poor oxidation potentials of these oxidants, so a long treatment time is required. Dye sometimes can slowly degrade to produce other pollutants that can also cause environmental issues [26]. Therefore, there is a need to discover new materials with higher oxidation potentials to treat dye wastewater.

All these factors have led scientists to search for new methods to preserve the environment and for sustainable eco-friendly development.

These new methods include advanced oxidative processes (AOPs). AOPs are efficient wastewater treatment techniques to degrade organic substances by producing reactive oxygen species (ROS) including superoxide ($\cdot O_2^-$) and hydroxyl ($\cdot OH$) radicals. They are prominent ROS with oxidation potentials of -2.3 and 2.7 eV vs. normal hydrogen electrode (NHE), respectively [27]. Generally, organic compounds have the oxidation potential from −1 to 2 eV vs. NHE. This difference in potential between organic species and ROS, makes an organic molecule entering a reactor containing ROS either to lose or gain electrons instantly and convert into two or more smaller composite parts [27]. Excellent removal performance of photocatalytic degradation is provided by the high redox potential of ROS. A comparative study of the degradation potential of a regular chemical treatment and of AOPs revealed that AOP eliminated 90% of COD while the chemical treatment removed 60% [28].

Fenton reaction and photocatalysis are two examples of AOPs used to degrade organic dye molecules [33]. Hydroxyl radicals ($\cdot OH$) are produced during the Fenton process. Then, these radicals degrade organic dyes into carbon dioxide and water. Nevertheless, this process has some disadvantages, including generation of waste sludge, requiring large amounts of reagents to be used and secondary contamination issues [34].

Photocatalysis is the AOP for removing dye molecules by degradation under ultraviolet (UV) and/or visible light energy to produce electron-hole pairs that can destroy dyes. Under light, semiconductor-based photocatalysts absorb photons, converting dyes into non-toxic carbon dioxide and water molecules. The photocatalysis technique is more attractive because of its low cost, efficiency, ease of processing and versatility and because it is an environmentally friendly process for wastewater treatment. Photocatalysts can be recycled after each water purification cycle, thus not generating any excess waste material. Furthermore, it does not require any temperature manipulations and provides complete mineralization [29,30]. However, photocatalysis has its limitations, such as the need for improved charge separation and carrier recombination problems.

A great advantage of this method is that sunlight illumination can be used in the photocatalysis process as the energy source. Each year, the sun delivers approximately 3×10^{24} J of clean, abundant and safe energy to the Earth's surface. The energy demand of all humans is four orders of magnitude smaller than this value. Thus, the utilization of sunlight energy to develop novel methods for wastewater treatment is becoming a crucial topic that attracts scientists from all over the world [31-33].

1.4 Photocatalysis mechanism

The general mechanism of the photocatalytic process involves absorption of photons and excitation of electrons from the valence band (VB) to the conduction band (CB) of a semiconductor material. Based on band gap theory, researchers have proposed various mechanisms for electron–hole generation, their transfer across the valence, forbidden energy, and conduction bands, and their recombination [34]. One of the well-adopted mechanisms for the photocatalysis is discussed in the following section (Fig. 1).

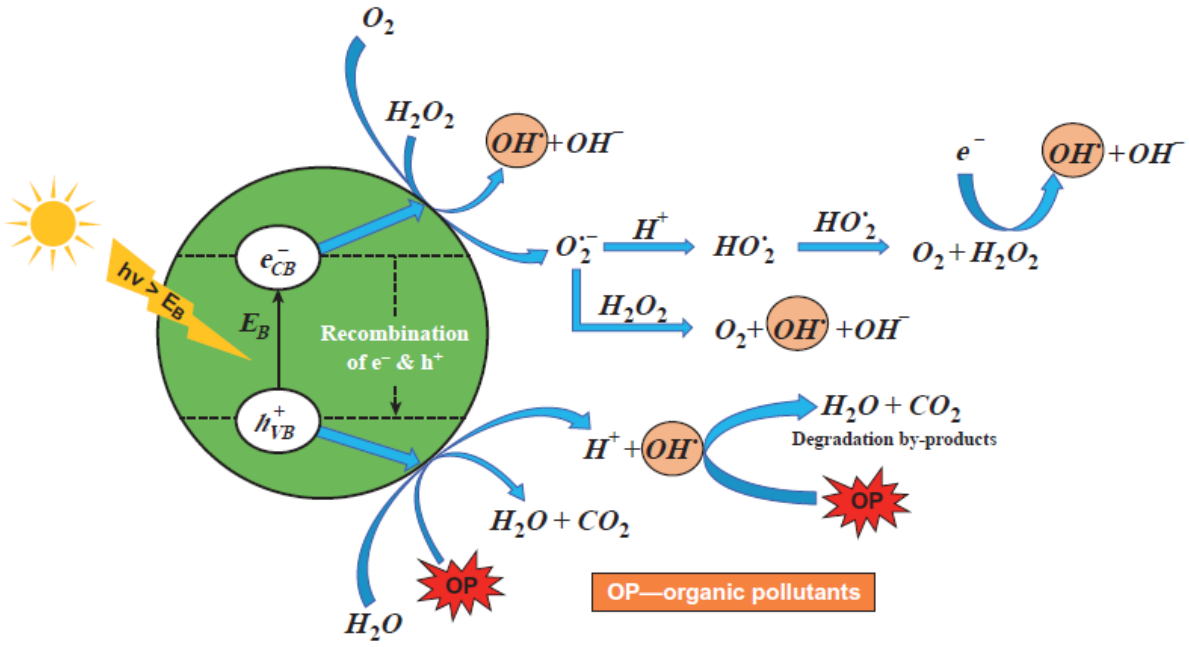

Fig. 1. Photocatalysis mechanism. Reprinted from [35]

Under ultraviolet (UV) and/or visible light, electrons (e^-) absorb light energy in the VB. If the incoming energy is greater than the bandgap energy, electrons will go from the VB to the CB. In this process, empty holes (h^+) will be left in the VB. From the CB, electrons can move to the surface of the photocatalyst to react with dissolved oxygen molecules, producing reactive oxygen species, which include superoxide radical $\cdot O_2^-$. At the same time, holes moving to the surface from the VB react with water molecules to give hydroxyl radicals ($\cdot OH$). Finally, holes themselves and both generated radicals oxidize organic dye molecules to produce intermediate species, which can be further oxidized to form carbon dioxide and water [35]. Notably, holes and electrons can recombine to produce heat as an energy. The overall photocatalysis reaction scheme can be written as follows:

$$\text{Photocatalyst} + h\nu \rightarrow h^+ + e^-$$

$$H_2O + h^+ \rightarrow \cdot OH + H^+$$

$$O_2 + e^- \rightarrow \cdot O_2^-$$

$$h^+ + e^- \rightarrow \text{Energy (heat)}$$

$$h^+ + \text{Pollutant} \rightarrow \text{Intermediates} \rightarrow H_2O + CO_2$$

$$\cdot OH + \text{Pollutant} \rightarrow \text{Intermediates} \rightarrow H_2O + CO_2$$

$$\cdot O_2^- + \text{Pollutant} \rightarrow \text{Intermediates} \rightarrow H_2O + CO_2$$

1.5 Influencing factors

There are, however, some problems related to semiconductor materials, including aggregate formation that consequently leads to a reduction in surface area and a wide band gap preventing effective electron flow [36]. Therefore, it is a primary need to develop new photocatalysts to overcome the weaknesses of semiconductors.

Three main features need to be considered in a visible light-responsive photocatalytic system. First of all, the electronic structure, which determines the band structure of the photocatalysts

and their optical properties. The semiconductor material should be able to absorb visible light, and the band gap must be narrow enough so that it can be excited by visible light photons. The second crucial feature is the crystallinity of the semiconductor. High crystalline material has fewer defects, which is useful for lowering the electron-hole recombination rate. The final key feature is the surface character, which has a critical effect on surface chemical reactions such as reduction by photogenerated electrons and oxidation by photogenerated holes [37].

In addition, other features, such as the morphological architecture, material choice, and surface properties, must also be taken into account when making a stable and efficient visible light-responsive photocatalytic system [38,39]. Choosing the right semiconductor material is especially important because it determines the degree of the visible light response and, therefore, the overall efficiency. The right morphology with a small distance between the redox reaction center and the photocarrier-generating junction can effectively enhance the carrier transportation and separation [40]. The geometrical shape and porosity of the photocatalyst determine its surface area. It has a critical impact on the photocatalytic activity because the adsorption of pollutant molecules is a crucial step in the photocatalytic process [41].

1.5.1 Band gap

Dye degradation efficiency highly depends on the band structure of the photocatalysts. The wavelength of the photons that can be received by the semiconductor photocatalyst is dependent on the band gap energy. Band gap energy, in turn, defines the range of wavelengths to be harvested and the photonic efficiency during the photocatalytic degradation reactions [42]. In addition, the band edge positions of the CB and VB are another crucial factor that influence the photocatalysis efficiency (Fig. 2). The band edge positions specify the thermodynamic limitations for the light induced reactions and can define the redox capacity of the generated electrons and holes. If the position of the VB is more positive than the potential of the redox couple, oxidation occurs, while more negative CB gives rise to a reduction reaction [43,44].

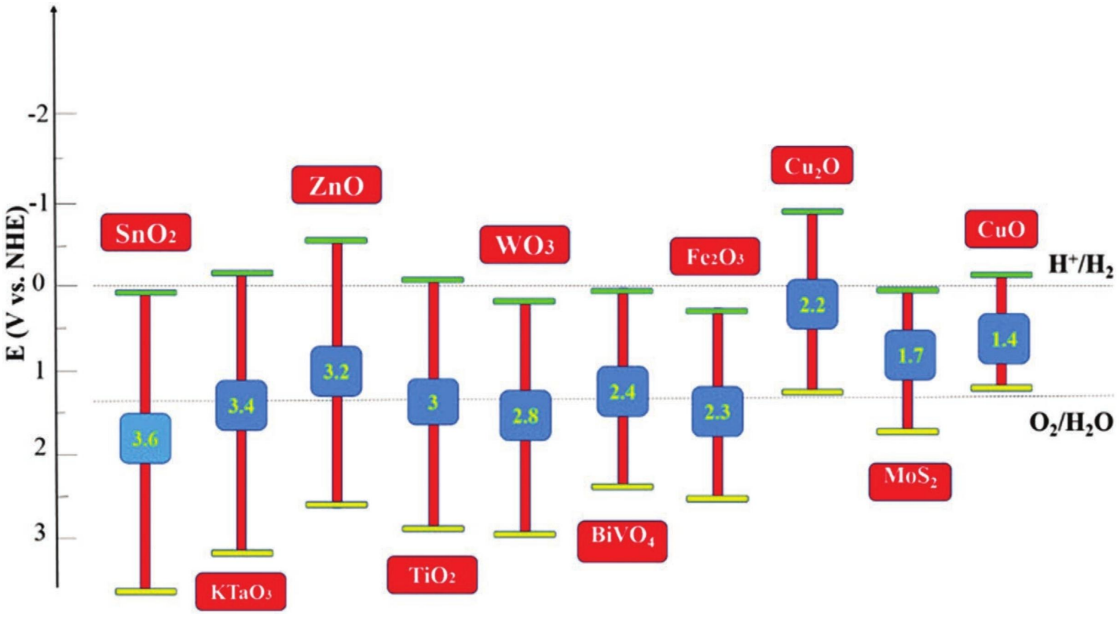

Fig. 2. Band gap and band edge positions of semiconductors. Reprinted from [45]

Particle shape and size influence the rate of reactions because they change the size of the band gap and the diffusion length of electron-hole pairs from the bulk to the surface-active sites. To maximize dye degradation, the band gap should not be too large (>3.0 eV) to be activated by the visible light nor be too small (<1.3 eV) to minimize the high probability of electron-hole pair recombination. In general, bandgap in the range of 1.3–3.0 eV has been reported to be suitable for photocatalysis [42].

1.5.2 Band gap engineering

The semiconductor photocatalyst material must have a small band gap to enable absorption of solar light energy across a broad range of spectra. Materials with large band gap energy can be doped to enhance their photoresponse. The bulk-doping method is based on the creation of allowed electronic states within the gap between the VB and the CB by incorporating dopants, such as nonmetal elements or metal ions. The electronic transition between bands of the semiconductor material and these states needs less energy compared to the band-to-band transition. Therefore, visible light photons can excite electrons and induce redox reactions [46].

A promising method to expand the photoresponse of a semiconductor material with a large band gap energy to the visible region of the spectrum is to harvest visible light photons by adsorbed color species such as dyes. In this method, the semiconductor material does not absorb light photons directly. Instead, adsorbed dye molecules function as antennae to absorb the light energy into the degradation system. The electron injection from the excited states of the adsorbed dye molecules into the CB of the semiconductor material can induce photochemical reactions [46].

First photochemical reaction was used in wide-band-gap silver halide (AgCl) photography. In the presence of dyes, AgCl emulsion was discovered to show a photographic response at longer wavelengths than the absorption onset of AgCl itself because of the visible light absorption by organic dyes. In 1977, Watanabe and coworkers [47] first investigated that electron transfer from the adsorbed rhodamine B dye in its singlet excited state to the CB of cadmium sulfide could bring to effective photochemical N-deethylation of the dye. Kamat et al. [46,48] reported that irradiation by visible light could cause the bleaching of adsorbed azo dyes on titania particles in the presence of oxygen.

1.5.3 Charge mobility and material stability

Improving charge mobility and charge carrier lifetime are other essential issues that should be considered in semiconductor photocatalysts [49–51]. Since photogenerated electron-hole pairs are amenable to recombination, increasing their mobility and separation time are worth attention in this regard. These factors can be examined through various routes to create heterojunctions by combining different semiconductors using novel morphologies, including defect introduction into the material, and porous structures. There are also some successful approaches for enhancing charge mobility in the structure of the semiconductor material and surface reactions with dye molecules, for example, incorporating conducting materials such as graphene or improving the crystallinity. To stimulate charge transfer in the interface between the dye and photocatalyst, special surface treatments or coatings can be conducted [52-54].

For photocatalysts, corrosion resistance and stability in aqueous solution are primary prerequisites. Furthermore, the photocatalyst must be stable during absorption of light and potential fluctuation. These barriers can be overcome through different methods. One example is

that the photocatalyst can be coated with highly stable materials against protons. Modification of the semiconductor material structure is another method that can be considered [53,55,56].

1.5.4 Catalyst loading

The mass of a photocatalyst has a substantial effect on the reaction rate and total dye degradation capability. Increasing the photocatalyst loading creates more electron–hole pairs, resulting in faster and higher degree of degradation. However, it was reported [57-59] that the amount of catalyst will not affect the rate of degradation directly. After a certain point, an increase in rate stops and can even decrease due to the lowering of the amount of active radicals that are produced by photoexcitation of a catalyst [60]. In a common sense, as more catalyst is present, more active sites should be present. However, after the optimum concentration, catalyst particles start to agglomerate, thus decreasing the surface area of the catalyst, which will lower the number of available active sites. Increasing photocatalyst loading leads to increased turbidity. Furthermore, suspension can be formed that blocks radiation from passing through, thereby increasing light scattering and reducing its penetration into the reaction mixture [61,62] which also, in turn, decreases the number of active surface sites, thus reducing the rate of dye degradation [63].

Lu et al. reported that the removal degree of rhodamine B dye increased with increasing amounts of a CdS/graphene composite photocatalyst in a reaction mixture. The removal degree went up from 49.1% to 84.5% when the amount of photocatalyst increased from 200 to 1800 mg/L [64]. Recently, another negative influence of higher photocatalyst loading on degradation efficiency was reported [65]. The degradation degree of para-nitrophenol was monitored against initial photocatalyst concentrations of 0.05, 0.15, 0.25, 0.35, and 0.45 g/L. The best removal performance of 97% was achieved at a concentration of 0.25 g/L. Further increase in concentration to 0.35 or 0.45 g/L decreased the removal degree. This decrease in photocatalytic performance was associated with increased light scattering and reduced penetration because of a high photocatalyst density per volume.

1.5.5 Dye loading

The interaction between a dye molecule and a photocatalyst particle is related to the amount of dye and the nature of the functional groups of the dye molecule. Generally, as the initial dye concentration increases, the degradation efficiency drops due to the competition of dye molecules for limited active sites. Moreover, a high dye loading makes the dye itself absorb more light than a photocatalyst particle, thus decreasing degradation performance [66]. The optimal concentration of a dye is highly dependent on its type and structure. Higher loading of methyl orange dye made fewer photons reach the photocatalyst surface because of light penetration decrease [67]. The effect of the loading of acid red dye on the degradation efficiency was also examined. The photocatalytic dye degradation rate dropped when the dye concentration raised from 20 to 40 mg/L. Increased dye loading hindered the photons from reaching the photocatalyst surface, inhibiting the production of ROS that decreases dye degradation performance [68].

1.5.6 Dye adsorption

The adsorption of dyes on the surface of a photocatalyst is dependent on the binding affinity and electrostatic interactions between the photocatalyst surface and the dye molecule [69]. Reasonable adsorption of dye molecules on the surface of a photocatalyst is helpful for degradation efficiency based on the synergy between photocatalysis and adsorption. The adsorption of dye molecules on the photocatalyst surface is an essential step for efficient photocatalytic degradation. The organic constituent of the basic dyes is positively charged in the solution. Positive charge allows dye molecules to adsorb readily on the surface of the photocatalyst with a negatively charged part. In the case of methylene blue dye degradation, it was observed that the TiO_2 photocatalyst removed from the reactor was blue-colored [70].

Photocatalysts with good adsorption properties simultaneously adsorb and degrade dye molecules taking advantage of the synergy principle [65]. TiO_2 incorporated graphene oxide resulted in a 50% enhancement in the methylene blue dye degradation compared to TiO_2 itself [71]. While adsorption of dye molecules on the photocatalyst surface is important for degradation, it may have adverse effects beyond a certain level. A very high number of adsorbed dye molecules on the photocatalyst surface decreases the number of photons reaching active

sites. Additionally, dye molecules can also act as sensitizers that absorb electrons and scatter them in unwanted directions [72].

1.5.7 Light intensity

Photocatalysis depends on the energy supplied by light photons. The light intensity plays a crucial role in photocatalytic dye degradation [75]. Electron–hole pairs are generated in the VB and CB of a photocatalyst when they get photons with energy equal to or greater than the band gap it has [73, 74]. The effect of light intensity on reactive yellow azo dye containing wastewater has been studied [76]. When the light intensity rised from 16 to 62 W/m^2, dye decolorization increased by 33%. A rise in irradiation power enabled enhancements in the penetration of light and an increase in the ROS generation rate. However, the rise in irradiation intensity enhances photocatalytic dye degradation degree only up to a certain level. Dye removal increases significantly when the light intensity rised from 16 to 32 W/m^2. A following increase from 32 to 48 W/m^2 provided very small change in dye degradation degree. Beyond that irradiation power, the dye degradation becomes independent of the light intensity.

The effect of irradiation power on degradation rate in the degradation of Fast Green dye was studied [77]. A linear growth in the kinetic rate constant was seen with an increase in the irradiation power. The results demonstrated that the kinetic rate constant nearly doubled as the intensity rised from 10 to 70 mW/cm. In a different study, an inverse effect of irradiation power on the Congo Red dye degradation rate was seen when the light intensity energy shifted from 50 to 90 J/cm [78]. The dye degradation rate increased with light intensity energy up to 80 J/cm. However, at 90 J/cm, the removal rate began to decrease, which should be attributed to the thermal effects related to the rise in temperature of the solution.

1.5.8 Temperature

Experimental investigation on the relation of the degradation rate of organic dyes to temperature has also been studied. Many researchers have reported the impact of temperature on photocatalytic activity [79–82]. Generally, raising the temperature increases the recombination

rate of electron-hole pairs and the desorption of adsorbed reactant species, thus decreasing photocatalytic activity. This observation is in accordance with the Arrhenius equation, for which the apparent first-order rate constant K_{app} increases linearly with exp(−1/T) [83].

1.5.9 pH of solution

The pH has a great effect on the photodegradation efficiency of dyes. The variation in solution pH changes the surface charge of a photocatalyst particle and shifts the potentials of catalytic reactions. As a result, the adsorption of dye on the surface changes thereby causing a change in the reaction rate. For example, under acidic or alkaline conditions, the surface of titania can be protonated or deprotonated, respectively, according to the following reactions:

$$TiOH + H^{+} \rightarrow TiOH_2^{+}$$

$$TiOH + OH^{-} \rightarrow TiO^{-} + H_2O$$

Every dye molecule has its own correlation with the change in pH of the environment [84]. That is why there is no ultimate guideline that can work with each dye. Moreover, in industrial processes, wastewater effluent typically consists of dye mixtures from different wet processes that have different pH values. Therefore, a single dye molecule cannot represent the actual properties of wastewater.

The pH of dye containing wastewater governs the electrostatic interaction between dye molecules, catalyst surfaces, and radicals during the degradation process. The surface charge and aggregation of the catalyst particles are related to the pH of wastewater [62,4]. Gaya et al. studied the impact of pH on the degradation capability of TiO_2 [85]. They have noticed that TiO_2 particles show weak photocatalytic degradation performance; the reaction rate decreased when the pH was less than 2.

In general, the following processes occur during the degradation of dye molecules under acidic conditions: High concentrations of H^+ ions interact with oxygen atoms in the conjugation system of the dye, thus altering its properties. Absorbance is typically lowered in acidic conditions. Under acidic conditions, holes are proposed to be accountable for the photoexcitation process.

Some studies have reported that there is significant adsorption of the dye on the catalyst under acidic pH, especially in the range of 1-3, which can be observed visually [86].

Under basic conditions, hydroxide ions (OH^-) and holes can react to produce hydroxyl radicals on the surface of the catalyst. These radicals are thought to be the main driving component of the photooxidation process. However, if the catalyst surface is negatively charged, inhibition of the hydroxyl radical formation can occur due to Coulombic repulsion between the OH^- and the catalyst surface [87].

1.5.10 Additives

The photocatalytic removal of organic dyes is also influenced by the presence of additives in the solution matrix [88-90]. In general, these additives are present as ions that are originally added to the dye solution as ionic compounds to enhance the industrial process but upon the release of wastewater, ions become an integral part of the effluent. Many common ions present in dye wastewater are Zn^{2+}, Ag^+, Fe^{2+}, Na^+, Cl^-, SO_4^{2-}, CO_3^{2-}, PO_4^{3-}, HCO_3^-, BrO_3^-, and persulfate ions. Each of these added ions induces some decrease in the degradation degree of the dye. For example, Fe^{2+} ions apparently undergo the following chemical reaction with generated hydroxyl radicals:

$$\cdot OH + Fe^{2+} \rightarrow OH + Fe^{3+}$$

This reaction has a considerably high rate constant value of 3.5×10^8 M/s [91]. Therefore, in the presence of Fe^{2+}, hydroxyl radicals are easily converted into hydroxides, thus lowering their concentration, and consequently less degradation of the dye is seen.

On the whole, metal ions are adsorbed onto the photocatalyst surface to make it slightly positively charged or electroneutral. As this process decreases the electrostatic repulsion for anionic dyes, they can be adsorbed and degraded easily in the presence of metal ions. Conversely, an inhibiting impact can also be seen for cationic dyes due to the reduction in attraction between slightly positive/neutral catalyst surfaces and positively charged dye molecules [68].

Photocatalysis is also affected by the presence of air or oxygen [90,92]. The degradation degree becomes less in the lack of oxygen, which has been attributed to the recombination of charge carriers. Oxygen molecules adsorbed on the surface of a photocatalyst inhibits the recombination by trapping electrons:

$$O_2 + e^- \rightarrow \cdot O_2^-$$

The degradation reaction rate is a function of the fraction of adsorption sites occupied by dissolved oxygen, thereby making it a limiting factor toward the photocatalytic process [93].

1.6 Overview of photocatalysts

For practical applications, using metal oxide nanostructures is considered to be a promising method for the photocatalytic degradation of organic pollutants. They include but are not limited to titanium dioxide (TiO_2, 3.2 eV), zinc oxide (ZnO, 3.3 eV), tin oxide (SnO_2, 3.6 eV), iron oxide (Fe_2O_3, 2.2 eV), strontium titanate ($SrTiO_3$, 3.4 eV), tungsten trioxide (WO_3, 2.8 eV), cadmium sulfide (CdS, 2.5 eV), zirconium dioxide (ZrO_2, 5.0 eV), zinc sulfide (ZnS, 3.6 eV), vanadium oxide (V_2O_5, 2.8 eV), ilmenite ($FeTiO_3$, 2.8 eV), and niobium pentoxide (Nb_2O_5, 3.4 eV) [94,95]. However, these photocatalysts generally have high band gap values that require the utilization of high-priced UV lamps for photoactivation. UV light from the sun only accounts for less than 10% of the total energy radiated and less than 5% of the solar energy that reaches the earth's surface. Moreover, the efficiency of these photocatalysts is still low because of other reasons, including recombination of electron-hole pairs, easy agglomeration, and problems in post-separation [96].

TiO_2 is one of the most known photocatalysts. It was first studied for the water splitting reaction [97]. Afterwards, its applications have been expanded to solar cells, hydrogen production, pollutant photooxidation, and dye degradation [98]. TiO_2 is extensively used as a photocatalyst due to its price, stability to photocorrosion, and inertness in chemical and biological environments. UV light generates electron‑hole pairs in TiO_2 structure for redox reactions due to a suitably sized band gap between its VB (+3.0 eV) and CB (–0.2 eV). Resulting band gap of 3.2 eV allows energy of near‑UV light with a wavelength shorter than 387 nm to produce electron‑hole pairs [15].

ZnO has been broadly used as a photocatalyst for decolorization of wastewater, due to its low cost, chemical stability, and large light absorption spectrum [27]. However, ZnO cannot be used for the photocatalytic degradation of pollutants because it dissolves in acidic solutions at low pH [58].

1.7 CuO photocatalyst

CuO is an intrinsically p-type narrow bandgap semiconductor that can be synthesized using chemical, biological, and physical techniques for various applications in different areas including in high-temperature superconductors, magnetic storage media, gas and chemical sensors, fuel cells, dye-sensitized solar cells, as an antimicrobial agent, and the degradation of pollutants in wastewater treatment. Due to its low price, easy availability, facile synthesis, narrow band gap (indirect, 1.2 eV), and superb photochemical stability, CuO has attracted attention for application in the photocatalytic removal of inorganic and organic contaminants [63]. The strong visible light absorption capacity of CuO makes it an extremely promising material for photocatalysis compared to other photoactive metal oxides [45]. Its structure can be seen in figure 3.

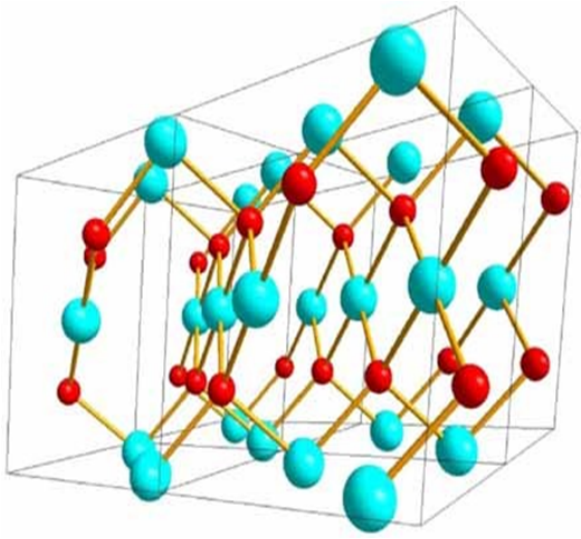

Fig. 3. CuO molecular structure. Reprinted from [101]

Different techniques have been investigated for the synthesis of nanostructured CuO, such as hydrothermal [102], microwave irradiation [103], sol-gel [104], solid-state reaction [105],

precipitation [106], sonochemical [107], and plasma [108]. Among these methods for CuO nanoparticle synthesis, the handiest are hydrothermal treatment, microwave irradiation, and precipitation. Each technique has its impact on the band gap and surface characteristics of CuO, such as the size of the particles, surface morphology, and specific surface area [45].

Compared to other metal oxides, CuO can be prepared with a variety of shapes (Fig. 4) that govern its catalytic, physicochemical, optoelectronic and antimicrobial properties [109]. For example, CuO in the shape of nanofibers [110], nanoflakes and microflowers [111], nanoparticles [112], and hexapods [113] have been extensively investigated for numerous applications.

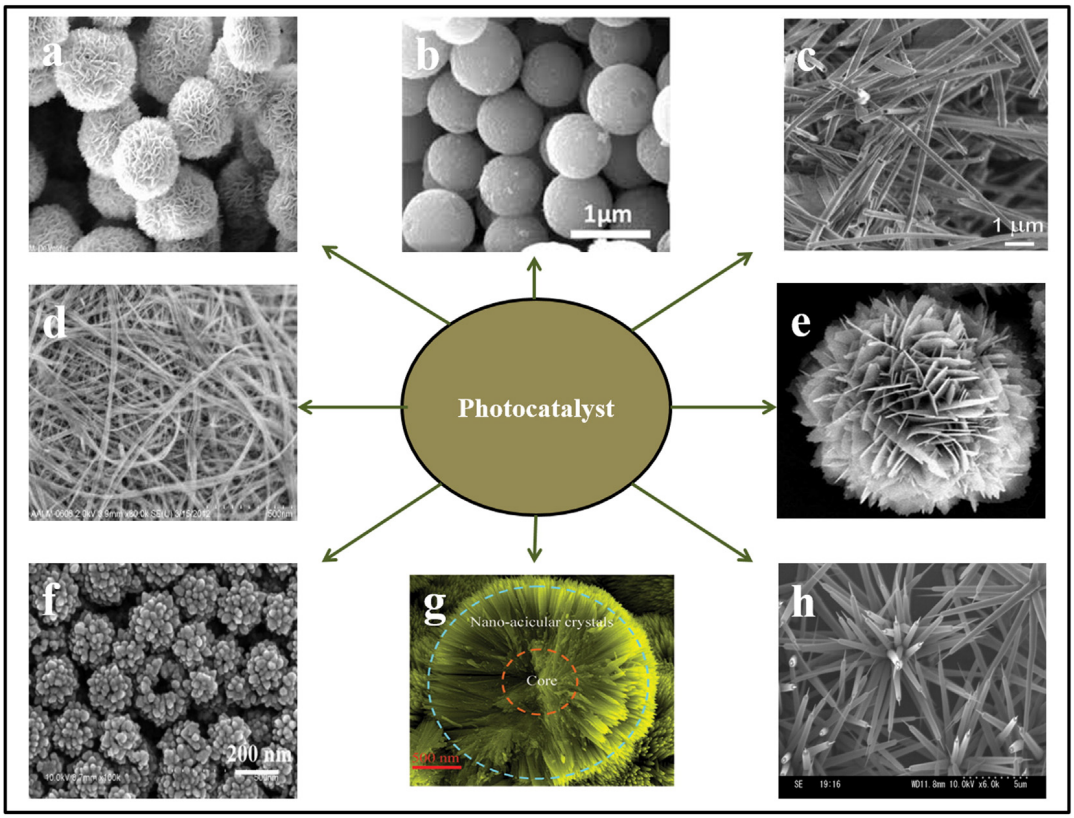

Fig. 4. Various CuO shapes. Reprinted from [114]

In addition to many excellent and unique properties, CuO has limitations, such as low band edge position. The high degree of electron-hole pair recombination due to its CB edge potential being more positive than the redox potential of hydrogen causes the low photocatalytic activity of CuO [63].

Several solutions indicated in previous reports, such as the formation of a heterojunction [115], modification with other elements, or doping [116], and controlling the morphology [117] are considered as suitable strategies to stimulate the photocatalytic activity of CuO. These practical methods can assist to overcome the limitations of CuO and enhance its performance by constituting one or more properties. These properties are increasing the specific surface area, lowering the activation energy, improving the charge separation, developing the electronic structure, and establishing novel mechanisms for the transmission of electron–hole pairs with the aid of bandgap engineering [118].

It should be noted that hydrogen peroxide is often added to the reaction mixture to enhance the photocatalytic activity of CuO. H_2O_2 is a better electron acceptor than O_2, thus it can be quickly reduced and converted to OH radicals after trapping e^- offering more active radicals. Moreover, it decreases the e^--h^+ recombination rate, thereby enhancing the overall photocatalytic efficiency of CuO. Without hydrogen peroxide, CuO itself was proved to be an ineffective photocatalyst, because it cannot produce sufficient amounts of OH radicals for degrading organic pollutants like dyes. The reason is that VBs of CuO are more negative than the potential needed to generate OH radicals, so they cannot generate OH radicals under solar light illumination. Different kinds of CuO nanostructures showed almost zero degradation after 15h of light irradiation in the absence of hydrogen peroxide [119].

Since the dye degradation mainly occurs on the surface of a photocatalyst, hollow CuO microspheres with a hierarchical morphology can effectively adsorb the dye on their surface resulting in improved degradation efficiency. Also, it is well-known that the hydroxyl radicals are the main active group in Fenton-like reactions. Thus, CuO microspheres can accelerate the decomposition of H_2O_2 and the generation of free radicals such as ·OH, ·OOH, and $\cdot O_2^-$. These free radicals attack the dye molecules resulting in their degradation. The reactions below describe the formation of these free radicals:

$$\text{photon} + \text{CuO} \rightarrow h_{vb} + e_{cb}$$

$$h_{vb} + H_2O_2 \rightarrow \cdot OOH + H^+$$

$$e_{cb} + H_2O_2 \rightarrow \cdot OH + OH^-$$

$$\cdot OOH \rightarrow \cdot O_2^- + H^+$$

1.8 Literature Review

Table 1. The efficiency of some CuO-based structures for rhodamine B degradation.

Photocatalyst type	RB dye conc.	Photocatalyst to dye volume ratio	H_2O_2 volume / 1 mg photocatalyst	Time/degradation percentage	Reference
Porous CuO microspheres	2.0×10^{-5} M	1 mg per 2.5 ml	0.25 ml (30 wt%)	60 min / 98%	Gu et al [120].
CuO nanosheets	1.0×10^{-5} M	1 mg per 2.5 ml	0.25 ml (30 wt%)	100 min / 93.4%	Wang et al [121].
CuO nanofibers	2.1×10^{-5} M	1 mg per 10 ml	0.04 ml (15 wt%)	160 min / 96%	Zeng et al [122].
CuO micro-particles	3.2×10^{-5} M	1 mg per 2 ml	0.02 ml (3 wt%)	90 min / 97.8%	Li et al [123].
CuO dendrites	2.0×10^{-5} M	1 mg per 2.5 ml	0.025 ml (30 wt%)	160 min / 80%	Yang et al [124].

Table 2. The efficiency of some CuO-based structures for methylene blue degradation.

Photocatalyst type	MB dye conc.	Photocatalyst to dye volume ratio	H_2O_2 volume / 1 mg photocatalyst	Time/degradation percentage	Reference
CuO flower-like lamellar	2.0×10^{-5} M	1 mg per 1 ml	0.02 ml (30 wt%)	240 min / 96.4%	Liu et al [125].
CuO bud-shaped	1.0×10^{-5} M	1 mg per 1 ml	0.02 ml (30 wt%)	120 min / 61%	Sorekine et al [126].
3D flower-like CuO	1.0×10^{-5} M	1 mg per 5 ml	1.00 ml (30 wt%)	210 min / 99.6%	Liu et al [127].
CuO nano-sheets	2.5×10^{-5} M	1 mg per 3.3 ml	0.33 ml (30 wt%)	30 min / 100%	Lobna et al [128].
CuO nanopetals	5.0×10^{-5} M	1 mg per 4 ml	0.05 ml (30 wt%)	30 min / 100%	Yang et al [129].

The tables above compare the efficiency of various CuO structures available in the literature for RB and MB degradation by taking into account several factors such as dye concentration, photocatalyst to dye volume ratio, H_2O_2 amount, degradation percentage, and time. Among the selected articles, dye degradation percentage varied between 61 and 100%, while the analyzed degradation time was between 30 and 240 min. Only five articles contained detailed experimental data for CuO-assisted photocatalysis in the presence of hydrogen peroxide. For the preparation of photocatalysts, mainly hydrothermal method was used in which copper nitrate hydrates acted as a precursor material for copper oxide. By varying the pH of the solution by adding ammonia or citric acid different structures of CuO were obtained. In the selected articles, X-ray Diffractometer (XRD), Energy Dispersive X-ray (EDX), Scanning Electron Microscope (SEM), and Transmission Electron Microscope (TEM) were used for photocatalyst characterization. XRD provided crystal structure and EDX analysis gave information about the elemental composition of the material. Both SEM and TEM were used for the imaging of micro and nanosized particles. To evaluate the photocatalytic activity of copper oxide mainly UV-Vis spectrophotometer apparatus was used to track the change in absorbance after a certain period of time, and the calculation of rate constant was the choice in some studies. Organic dyes such as rhodamine B and methylene blue were mainly examined because they are one of the most used chemicals in industry. CuO showed many advantages like high degradation rate, high adsorption capacity, convenience in manipulation, and separation.

1.9 Aims of the present study

The objective of this project is to develop an environmentally friendly low-cost wastewater treatment system for use in the textile industry, using a CuO-based catalyst under irradiation by solar light. A systematic study of photocatalytic dye degradation using CuO catalysts and various types of industrially-relevant dyes was performed. Furthermore, the effect of altering the pH of the solution has been studied. Both commercially available and custom-made CuO were used as catalysts.

In addition, high-speed centrifugation and filtering techniques are typically required for NPs separation, which in turn increase the water treatment cost. Therefore, the fabrication of a photocatalyst that can be activated through solar light and rapidly eliminated from the solution is

fascinating both from technological and scientific points of view. Such a photocatalyst can be used for the photodegradation of organic pollutants directly below the solar light illumination, hence, decreasing the cost of a photocatalytic process. In addition, the preparation of larger-sized porous photocatalysts can potentially resolve problems associated with the separation processes. For example, large-sized porous photocatalysts have a high specific surface area appropriate for the photocatalytic processes and can be rapidly precipitated in the solution phase.

The formation of hollow microspheres with a hierarchical structure can grant an enlarged contact interface that is really useful for improved catalytic, electrochemical, and optoelectronic properties. Traditional techniques for the synthesis of hollow CuO microspheres typically depend on hard/soft template-based strategies that require harsh chemical substances for template elimination [130,131]. Regrettably, much less effort has been centered on creating uncomplicated protocols for the synthesis of CuO with a high specific surface area [132]. Hence, the development of a synthesis method that would be technically easy and cheap is of high scientific interest.

The aim of this research is to find a new potential application of CuO in photocatalytic dye degradation and to evaluate its structure-performance connection for potential usage on industrial scales. CuO-based photocatalyst will be investigated with respect to the effectiveness of the photocatalytic activities towards the degradation of RB and MB dyes in the aqueous solutions under a solar simulator light irradiation.

2. METHODOLOGY

2.1 Materials

$CuCl_2 \times 2H_2O$ (≥99.0%), cetyltrimethylammonium bromide (CTAB,≥99.0%), urea (99.0–100%), H_2O_2 solution (34.5-36.5%), methylene blue (MB, ≥95.0%), rhodamine B (RB, ≥95.0%), and commercial CuO (<50 nm particle size) had been purchased from Sigma-Aldrich and used as received. Commercial CuO was taken to compare with synthesized one.

2.2 Synthesis

2.2.1 CuO photocatalyst

For the synthesis of CuO, 0.2 g of $CuCl_2 \times 2H_2O$, 0.2 g of CTAB, and 0.3 g of urea were dissolved in 20 ml of deionized (DI) water. Then the obtained solution was transferred to a 50 ml Teflon-lined stainless steel autoclave. Next, the autoclave was heated in the muffle furnace at 160 °C for 5 h (ramping rate 5 °C/min). Formed precipitates were separated by the aid of a centrifuge, washed with DI water, and dried. Finally, obtained powder was calcinated in the muffle furnace at 400 °C for 30 min to obtain black-colored CuO microspheres.

2.2.2 Dye solutions

$1x10^{-5}$ M dye solutions were prepared by dissolving 1.9 mg of rhodamine B and 1.3 mg of methylene blue in 400 ml of DI water.

2.3 Sample characterization

The scanning electron microscope (SEM, Auriga Crossbeam 540) with Energy Dispersive X-ray EDX was used for morphology, size determination, and chemical analysis. The transmission

electron microscopy (TEM) image was recorded on a JEOL JEM-1400 Plus with an accelerating voltage of 120 kV. The crystalline phases of the samples were examined by means of X-ray Powder Diffraction using a Rigaku SmartLab X-ray Diffractometer (XRD) geared up with a Cu Kα radiation source. Autosorb iQ nitrogen porosimeter (Quantachrome Instruments) was used to determine the surface area and pore size distribution of CuO microspheres. LCS-100 solar simulator (100 W xenon lamp, AM1.5G filter) was used to perform the photodegradation of the dye solution (1×10^{-5} M). The distance was once optimized to supply 1 sun irradiance using a standard silicon-based reference cell. The photodegradation of RB and MB solutions versus irradiation time was monitored using UV-Vis (Genesys 50) spectrophotometer.

2.4 Photocatalytic activity test

Photocatalytic dye degradation was carried out using the "all-in" method, in which all reagents were mixed together before the solar simulator light irradiation. The photocatalytic activities of the photocatalyst were evaluated by adding 2 mg of CuO microspheres into 5 mL of dye solution ($1x10^{-5}$ M) in a glass beaker, and then stirring the mixture at 600 rpm for 10 min in the dark to establish an adsorption-desorption equilibrium. Finally, the H_2O_2 solution (0.01 mL) was added, and the light was turned on immediately. At the given irradiation time intervals, part of the solution was immediately taken by means of a syringe and filtered using a 100 nm filter to the cuvette. Then absorbance of the dye solution was once measured immediately. All experiments have been repeated three times to ensure the reproducibility of the results.

3. RESULTS & DISCUSSION

3.1 Morphological analysis

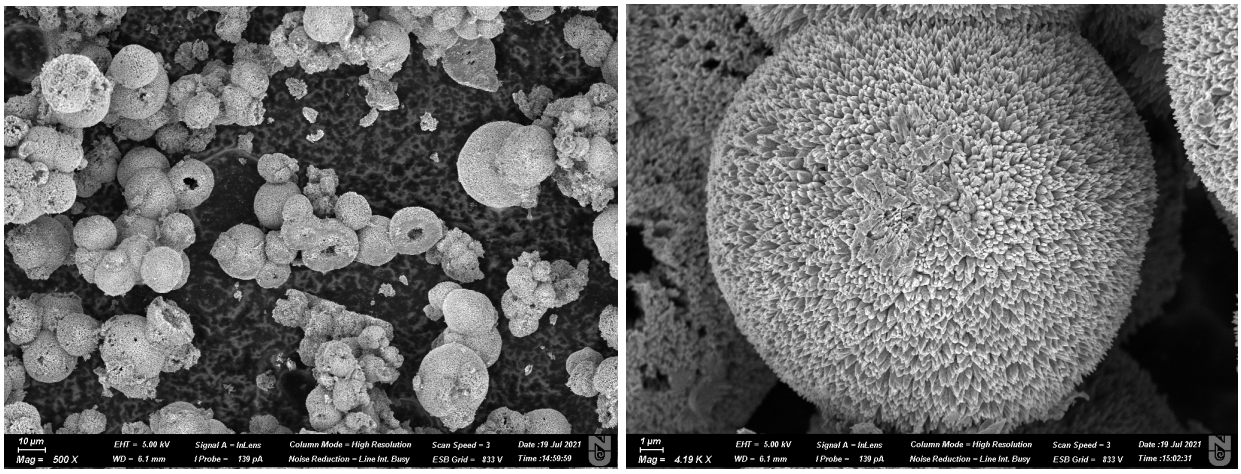

Fig. 5. Low-magnification SEM images of hollow CuO microspheres.

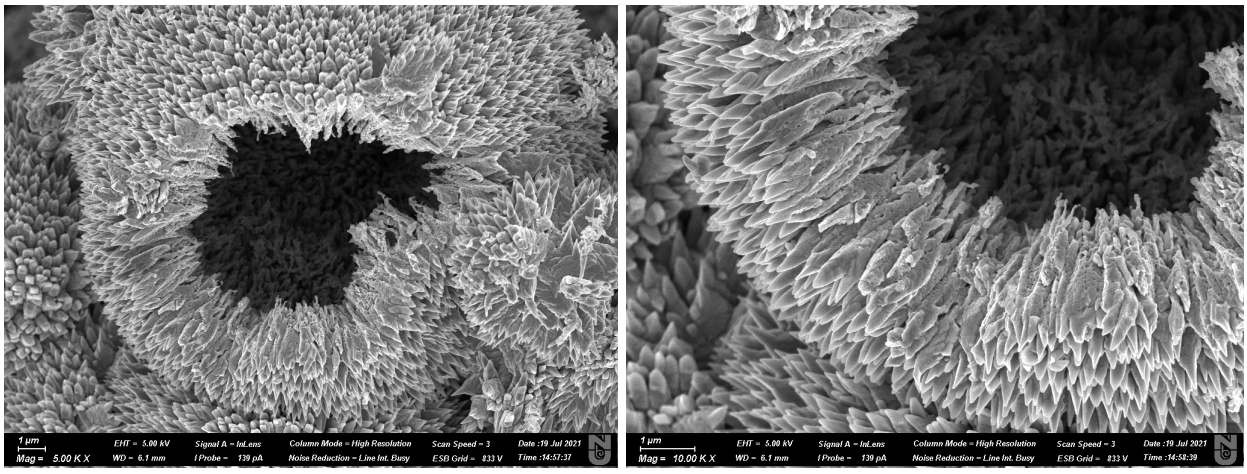

Fig. 6. Close up SEM images of hollow CuO microspheres.

Figures 5 and 6 represent SEM images of CuO with low and high magnification. By analyzing size and morphology, the shape of the microspheres was found to be quasi-spherical. The diameters of obtained microspheres were between 11 and 20 µm.

Images above and ruptured microspheres indicated that the microspheres were hollow-structured and they consisted of crystal strips directed to the center of microspheres. The length of crystal strips (i.e. the thickness of the microsphere wall) was found to be between ~ 1.12 – 1.67 µm.

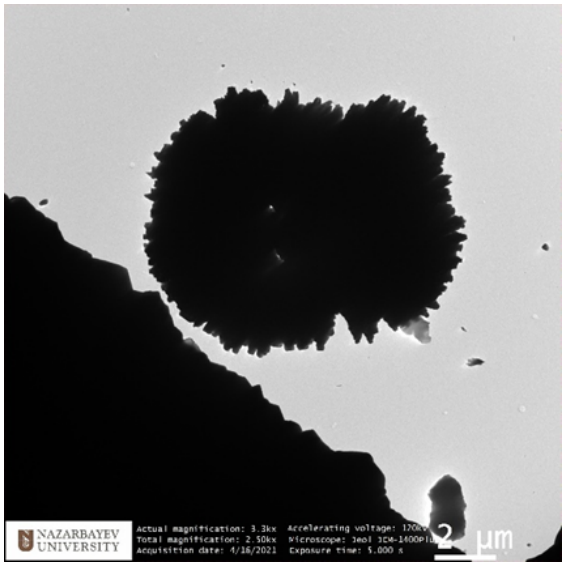

Fig. 7. TEM image of prepared CuO microspheres.

Figure 7 shows a TEM image of CuO microspheres. The hollow structure of CuO is not clearly visible because of the high wall thickness.

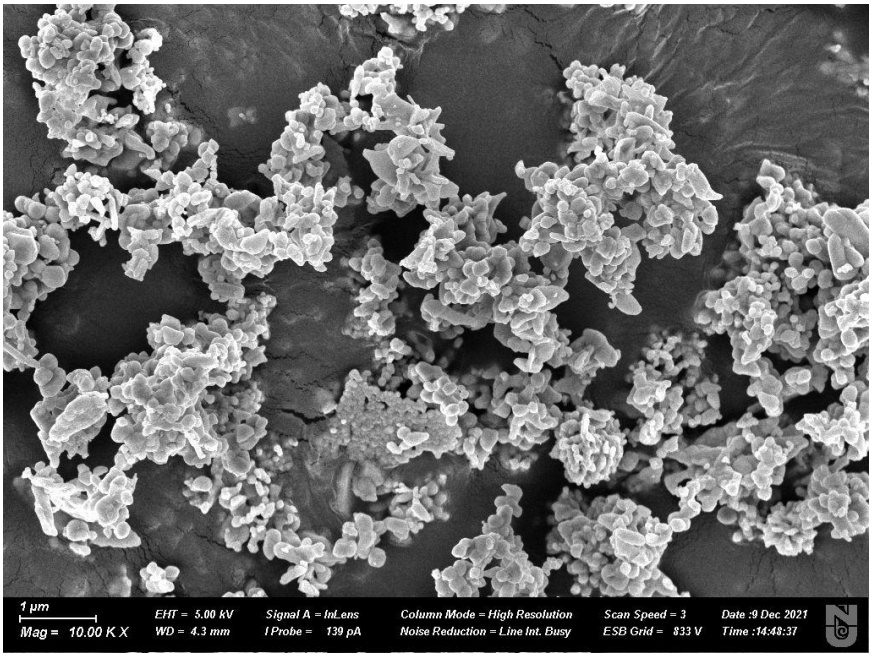

Fig. 8. SEM images of commercial CuO.

Figure 8 demonstrates the SEM image of purchased commercial CuO nanoparticles with the size less than the 50 nm.

3.2 Compositional analysis

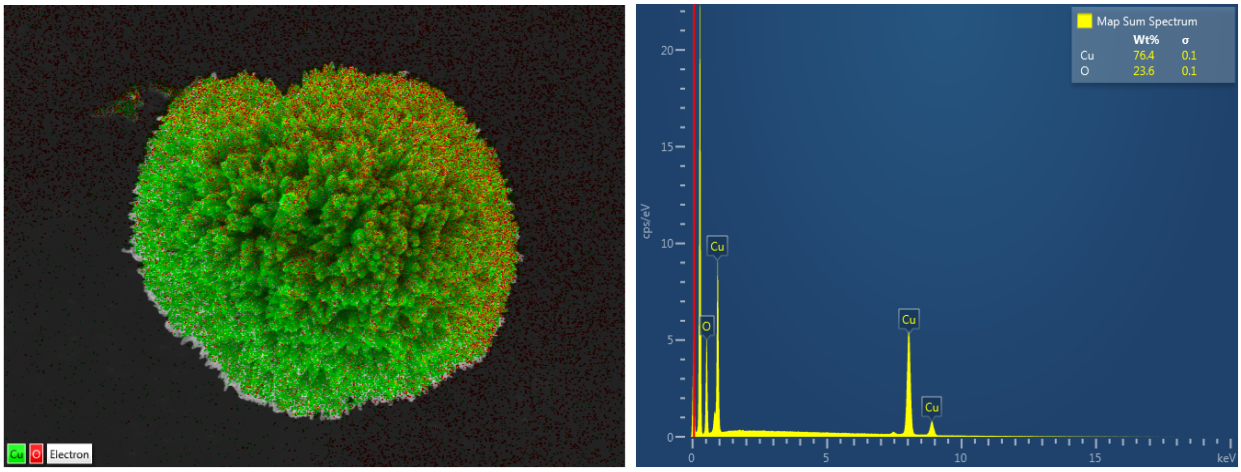

Fig. 9. Chemical analysis by EDX.

Figure 9 shows EDX images of obtained CuO microspheres. Chemical analysis indicated that the sample contained only copper (Cu) and oxygen (O) elements. According to EDX analysis, the concentration of Cu was found to be 76.4 % by weight, which is almost equal to the theoretical value of 79.9%.

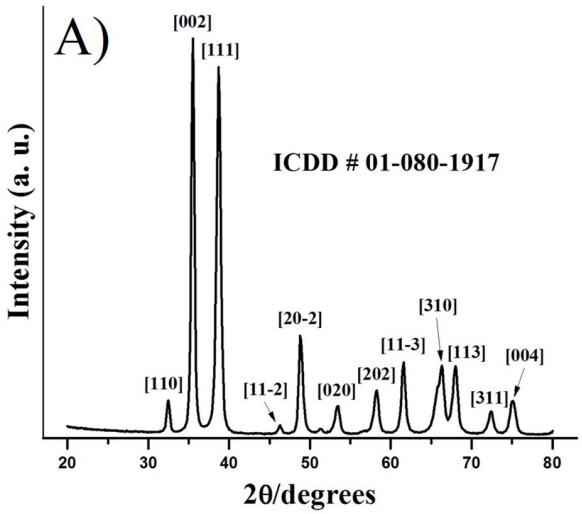

Fig. 10. XRD analysis of CuO.

Monoclinic CuO structure (ICDD#01–080-1917) well corresponds to the XRD pattern shown above. All peaks can be easily assigned. XRD analysis supports EDX analysis by showing no peaks from other elements, indicating that the sample is very pure.

3.3 Optical analysis

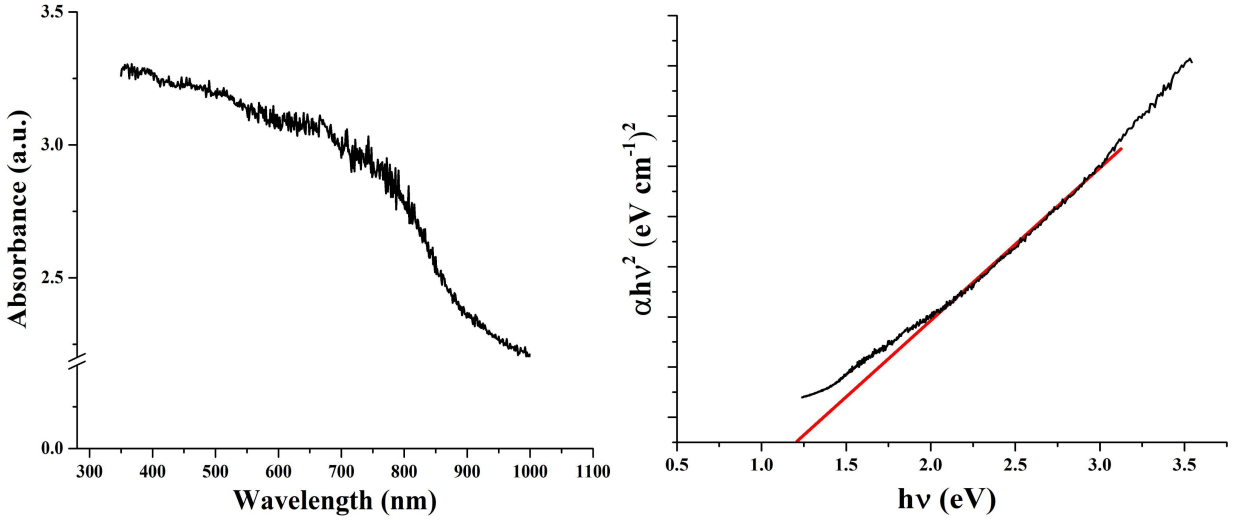

Fig. 11. (left) UV-Vis analysis of CuO and (right) indirect bandgap calculation.

UV-Vis spectroscopy was used to estimate the absorbance of CuO microspheres. Sample absorbed light in UV-NIR range (300-1000 nm).

Tauc plot was used to identify the band gap of CuO using the UV-Vis absorption data. The Davis-Mott equation was used in calculations:

$$ah\nu=K(h\nu - E_g)^n$$

where, a - absorption coefficient, h - Plank's constant, ν - frequency, K - absorption index, n=1/2 for direct, and n=2 for indirect bandgap. CuO has an indirect band gap, so n=2 was used for calculations. Band gap was found to be 1.23 eV, which is very close to bulk CuO with 1.2 eV.

3.4 BET and BJH analysis

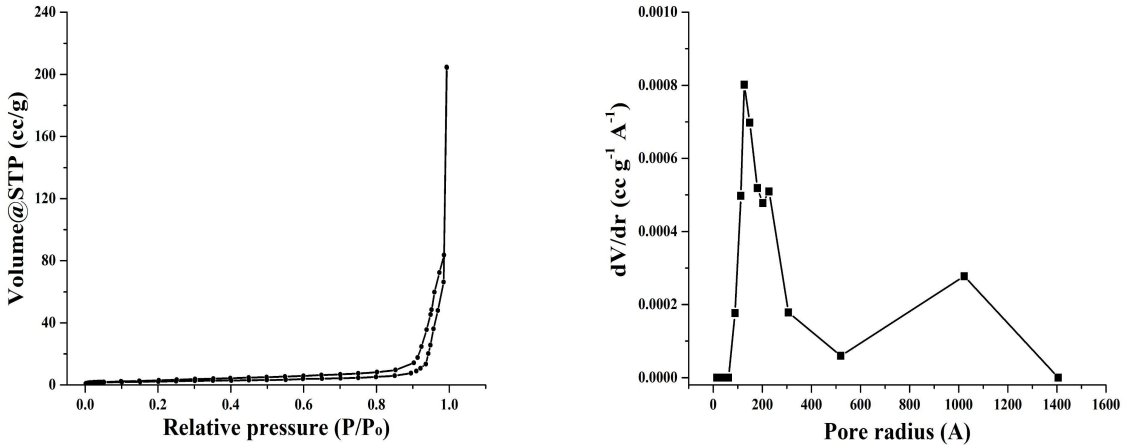

Fig. 12. (left) Nitrogen adsorption-desorption isotherms and (right) BJH pore size distribution.

It is seen that between 0.8–1.0P/Po type IV structure was formed with the H3 hysteresis loop. Thus, according to IUPAC classification, the presence of macropores and mesopores was shown. By BET analysis it was found that the surface area of CuO microspheres was 12.184 m^2/g. BJH method was used to analyze the pore size distribution in the sample. According to it macropores (d_{max} ~ 203 nm) and mesopores (d_{max} ~ 31 nm) coexist in the sample. The high distribution of micropores, represented by mesopores, confirms the samples' applicability in photocatalysis.

3.5 Photocatalytic activity analysis

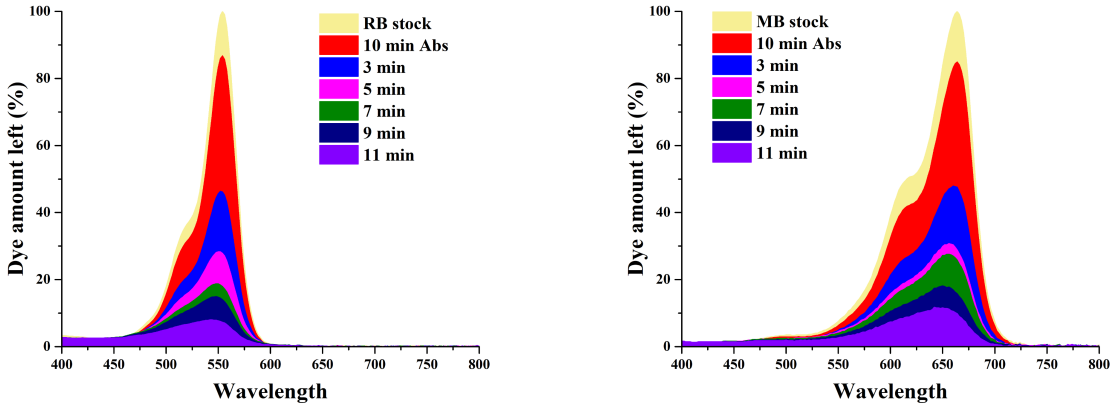

Fig. 13. Absorbance intensity of (left) RB and (right) MB with CuO + H_2O_2.

It is well-known that organic dyes can be partially adsorbed on the CuO surface while stirring in the dark. It was found that the adsorbed dye amount was ~ 15% for both RB and MB. Hence, the degradation start point was lower in measurements with CuO microspheres. RB has maximum absorbance at 554 nm, while MB at 664 nm. Absorbances at these wavelengths were used to calculate the degradation degree of dyes.

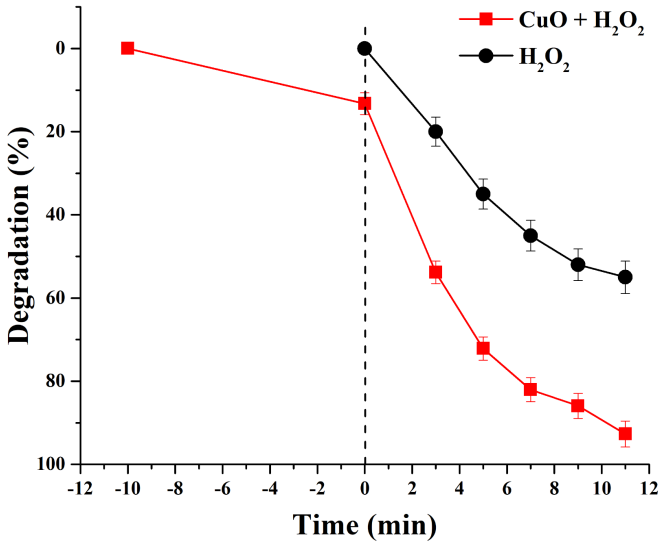

Fig. 14. RB degradation with (red) CuO + H_2O_2; (black) H_2O_2.

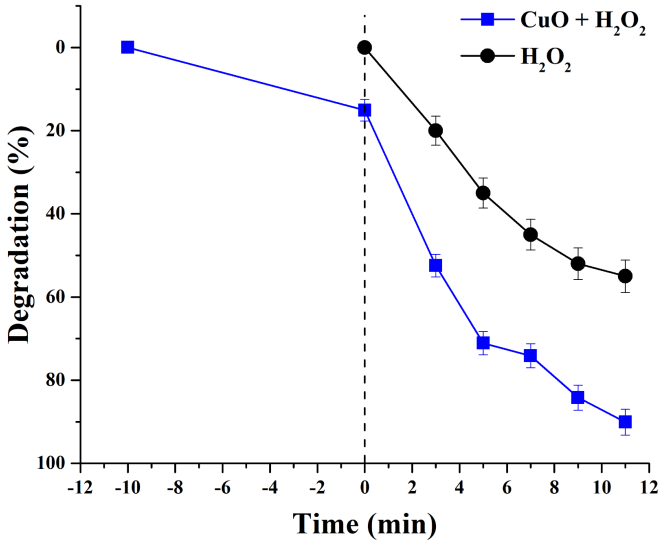

Fig. 15. MB degradation with (blue) CuO + H_2O_2 and (black) H_2O_2.

The change in dye concentration has been calculated according to the equation:

$$\text{Degradation (\%)} = (1-C_t/C_0) \times 100$$

By Beer's law, the concentration, and absorbance (A) are proportional, thus we can write the above equation as follows:

$$\text{Degradation (\%)} = (1-A_t/A_0) \times 100$$

Where A_t is the absorbance of the dye at any period of time (3/5/7/9/11 mins) and A_0 is the initial absorbance of the dye solution.

Photocatalysis was done in the presence of H_2O_2 because CuO itself cannot trigger it. H_2O_2 itself can degrade rhodamine b and methylene blue but degradation rates were significantly increased when it was used with the CuO microspheres. After 11 min, the degradation by only H_2O_2 reached a value of 55%, while the photodegradation rate in the presence of CuO and H_2O_2 significantly accelerated and reached a value of approximately 90% after 11 min for both dyes.

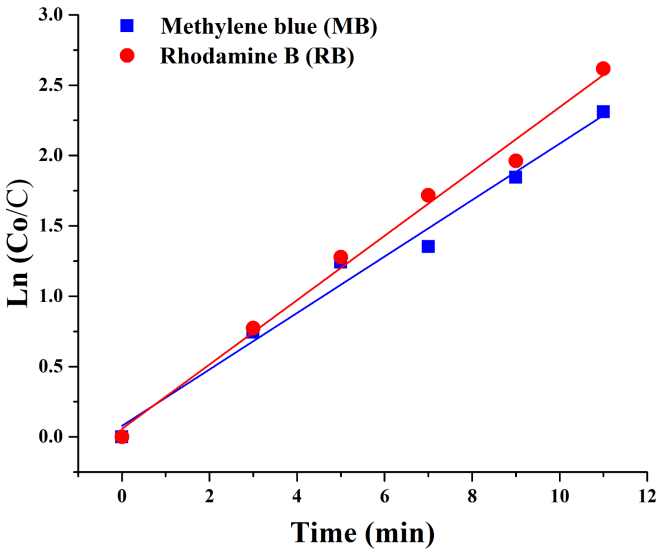

Fig. 16. CuO + H_2O_2 degradation kinetics for (blue) MB and (red) RB.

Degradation efficiency was further analyzed by plotting the linear fit between ln (C_0/C) and time (Fig. 16). To estimate the kinetic of the dye photodegradation, the following equation was used:

$$ln(C_0/C_t) = kt$$

where k is the degradation rate coefficient. Calculations yield the following average degradation rates:0.243/min for RhB and 0.221/min for MB.

3.5.1 Comparison with commercial CuO

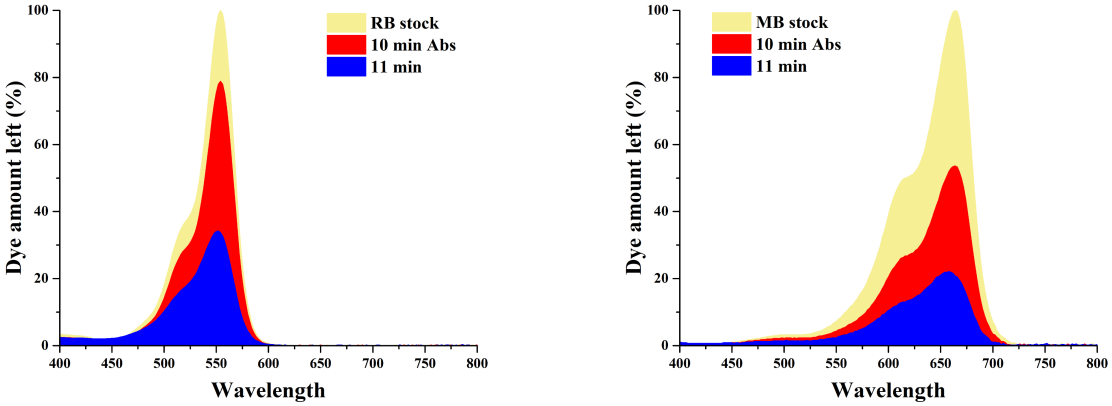

Fig. 17. Absorbance intensity of (left) RB and (right) MB with commercial CuO + H_2O_2.

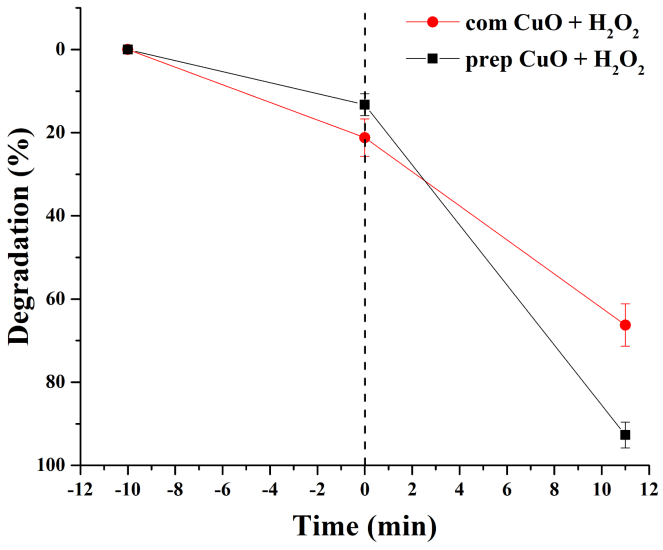

Fig. 18. RB degradation with (red) commercial CuO + H_2O_2 and (black) prepared CuO + H_2O_2.

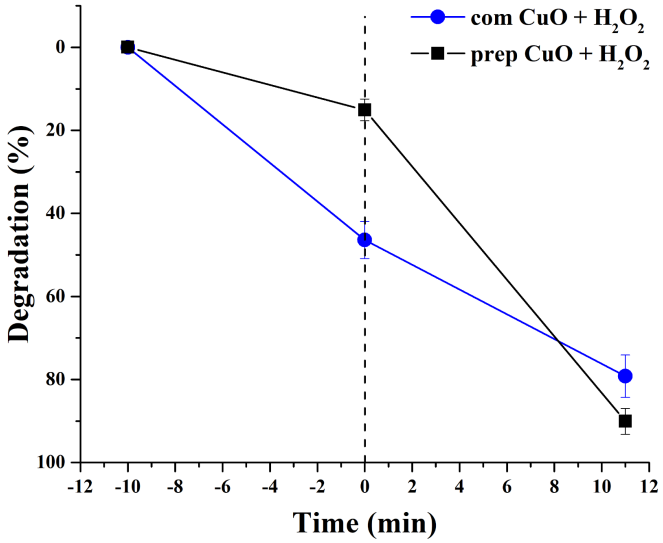

Fig. 19. MB degradation with (blue) commercial CuO + H_2O_2 and (black) prepared CuO + H_2O_2.

It is seen that commercially available CuO nanoparticles have lower effectiveness towards dye degradation. After 11 min, degradation degree was ~70% and ~80% for RB and MB, respectively. While commercial nanosized CuO with larger surface area should have a higher efficiency, prepared hollow CuO microspheres with crystal strips showed better results.

3.5.2 One-pot recyclability tests

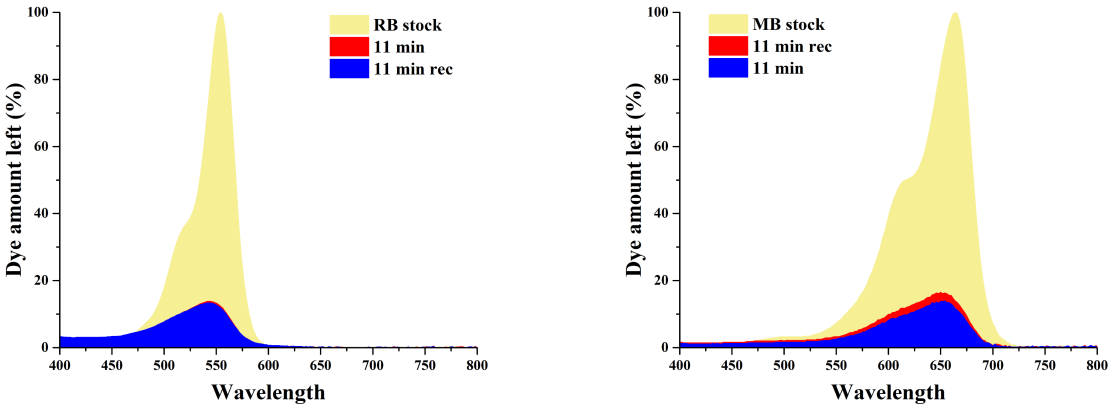

Fig. 20. Absorbance intensity of (left) RB and (right) MB with recycled CuO + H_2O_2.

To be truly industrially relevant, a photocatalyst must be reusable. It should be possible to recycle the photocatalyst after separating it from the product mixture for further photocatalytic reactions without a noticeable drop in performance.

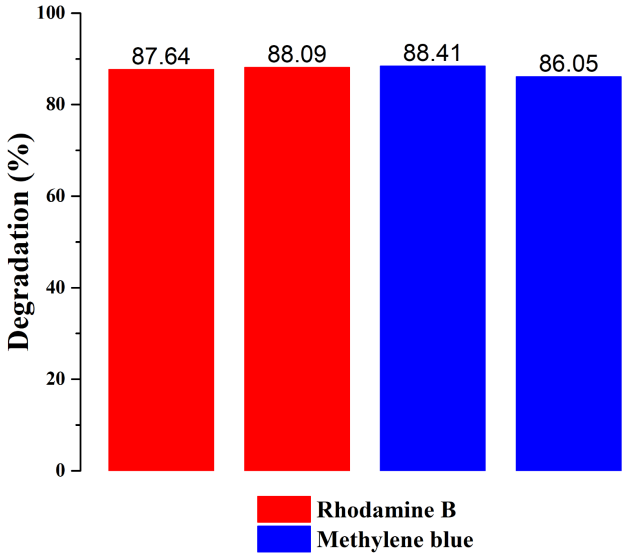

Fig. 21. Recyclability tests of (red) RB and (blue) MB.

After the first photocatalytic degradation reaction, the solution was taken by syringe, so that CuO was left on the bottom of the beaker. The recyclability test was done by pouring another 5 ml of dye and starting the process again. It is worth noting that these CuO microspheres due to their size can be quickly precipitated to the bottom of the flask making them easily recyclable. Recyclability analysis showed that CuO microspheres can be efficiently reused at least two times without losing efficiency.

3.5.3 Tests in acidic conditions

The stock solution of $1x10^{-5}$ M rhodamine B has a pH of 5.3 while the stock solution of $1x10^{-5}$ M methylene blue has a pH of 7.4. The pH of the solution was decreased by adding tiny drops of concentrated HCl, so that the total volume of the dye solution remains almost the same. pH was of the solution was measured by portable digital pH meter.

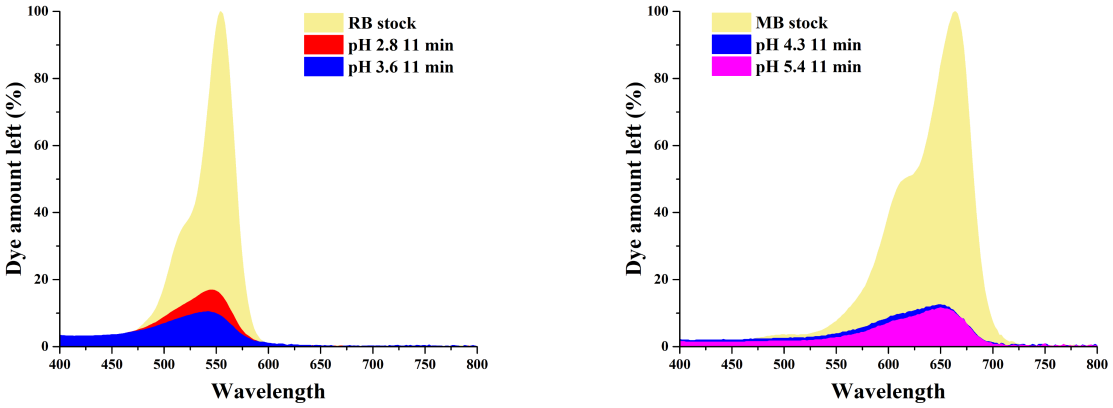

Fig. 22. Absorbance intensity of (left) RB and (right) MB with acidic CuO + H_2O_2 .

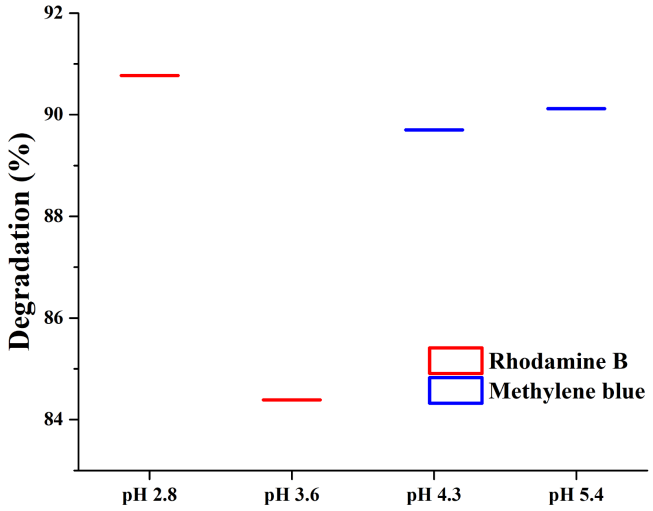

Fig. 23. Degradation of (red) RB and (blue) MB with CuO + H_2O_2 in acidic conditions.

At low pH, the degradation percentage of both dyes decreases. In general, the performance of photocatalytic degradation decreases with the drop in pH because H^+ ions adsorbed on the CuO surface make it positive. Both RB and MB are cationic dyes, so at low pH, there will be repulsion between the catalyst and dye molecules.

The concentration of the dyes was converted from their absorbance values using the constant extinction coefficient of each dye in pure water. With pH alteration, deviations in the concentrations can occur because of these different conditions, but the obtained converted concentrations are still comparable with their absorbance to a large degree.

3.5.4 Tests in basic conditions

The initial pH of RB and MB were 5.3 and 7.4, respectively. The pH of the solution was increased by adding tiny drops of concentrated NaOH solution, so that the total volume of the dye solution remains nearly unchanged.

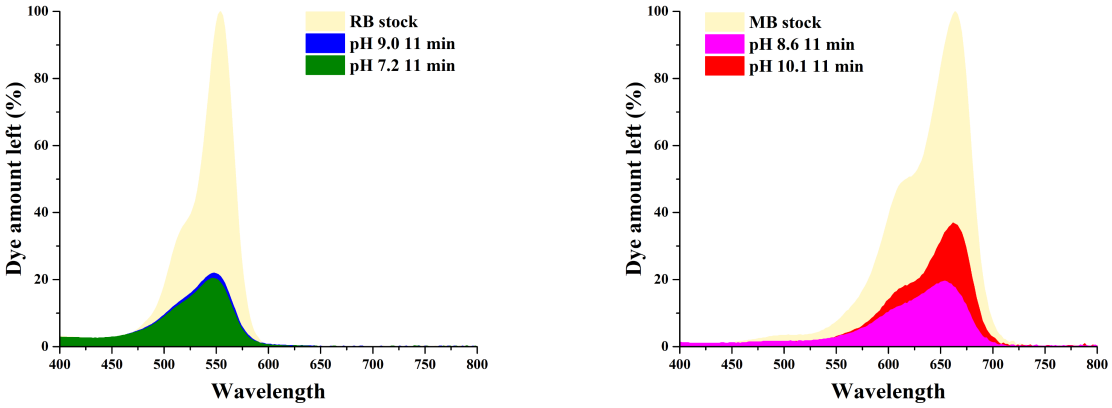

Fig. 24. Absorbance intensity of (left) RB and (right) MB with basic CuO + H_2O_2 .

At high pH, the degradation degree of both dyes also decreases. The reason is the formation of intramolecular hydrogen bonds at high pH values. Thereby, the dye structure becomes chemically stable at high pH ranges. The chromophores of the dye remain intact after light irradiation and hence decrease the degradation percentage of the dye [133].

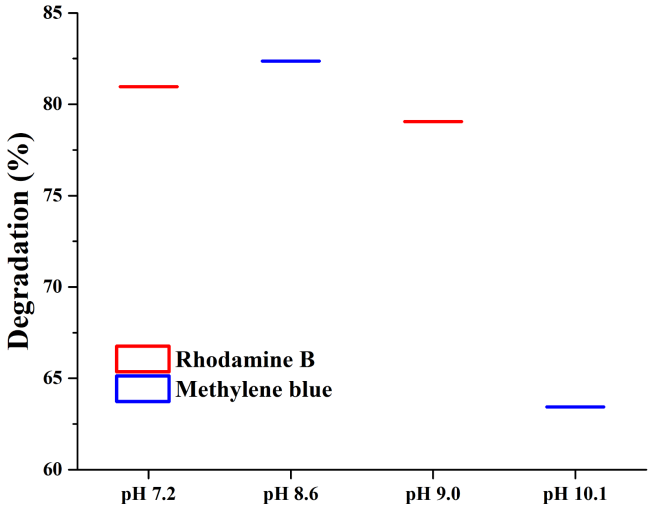

Fig. 25. Degradation of (red) RB and (blue) MB with CuO + H_2O_2 in basic conditions.

4. CONCLUSION

In summary, hollow CuO microspheres with diameters ~11–20 μm were prepared for potential solar light-activated degradation of model dyes with the assistance of H_2O_2. Dark absorbance for both dyes was at around 15%. We showed that synthesized CuO microspheres substantially accelerate the photocatalytic degradation rate of model dye under solar light irradiation reaching 90% degradation in 11 min. It is suggested that enhanced photocatalytic reaction was observed thanks to the synergy of two factors: accelerated formation of radical ions from H_2O_2 in the presence of CuO microspheres and high dye absorbance on the rough surface of CuO microspheres with the surface area of 12.184 m^2/g. The rate of photocatalysis is greatly influenced by the parameters of the system. In this study, it has been investigated that pH can impact the degradation rate by changing the surface charge and ionization properties of both the catalyst and the dye. Generally, at low and high pH values, reactions proceeded slower than those at almost neutral pH. To conclude, hollow CuO microspheres can be considered a promising material for wastewater treatment by the photocatalysis process.

5. LIMITATIONS & FURTHER STUDIES

Dye color removal does not surely match with the total elimination of dye, and other analytical methods such as Total organic carbon (TOC) or Gas chromatography-mass spectrometer (GC-MS) should be used to verify dye degradation percentage and to recognize the exact species resulting from the photocatalysis. This would help to identify dye degradation pathways. It should be noted that other than UV-Visible spectroscopy, the analyses were planned to involve TOC analysis and High-performance liquid chromatography-mass spectrometer (HPLC-MS). Unfortunately, the two last methods of analysis could not be performed because of technical reasons. TOC measurements data were unreliable, so they were not included in the current thesis. HPLC-MS system in block C4 (core facilities) was not working. Apart from that, this research is also limited by the time (M.Sc. study period).

Designing a suitable photocatalyst immobilization strategy to provide an inexpensive liquid-solid separation is a big challenge. At the current stage, one detrimental restriction is running out of catalysts during photocatalysis, which endangers the regeneration of the catalysts and poses adverse impacts on the environment. Immobilized photocatalysts can escape problems related to agglomeration, and catalyst recovery as well as minimizing reactor scale.

Based on existing information up to date, it is difficult to suggest a probable mechanism for hollow CuO microspheres formation. It is expected that the formation mechanism will be addressed in a future study. The application of photocatalysis to real wastewater processing is another interesting aspect to be investigated further.

6. REFERENCES

(1) Maruthupandy, M.; Qin, P.; Muneeswaran, T.; Rajivgandhi, G.; Quero, F.; Song, J. Graphene-Zinc Oxide Nanocomposites (G-Zno Ncs): Synthesis, Characterization And Their Photocatalytic Degradation Of Dye Molecules. *Materials Science and Engineering: B* **2020**, 254, 114516.

(2) Roşu, M.; Socaci, C.; Floare-Avram, V.; Borodi, G.; Pogăcean, F.; Coroş, M.; Măgeruşan, L.; Pruneanu, S. Photocatalytic Performance Of Graphene/Tio2-Ag Composites On Amaranth Dye Degradation. *Materials Chemistry and Physics* **2016**, 179, 232-241.

(3) Shanmugam, M.; Alsalme, A.; Alghamdi, A.; Jayavel, R. Enhanced Photocatalytic Performance Of The Graphene-V2O5 Nanocomposite In The Degradation Of Methylene Blue Dye Under Direct Sunlight. *ACS Applied Materials & Interfaces* **2015**, 7 (27), 14905-14911.

(4) Gaya, U.; Abdullah, A. Heterogeneous Photocatalytic Degradation Of Organic Contaminants Over Titanium Dioxide: A Review Of Fundamentals, Progress And Problems. *Journal of Photochemistry and Photobiology C: Photochemistry Reviews* **2008**, 9, 1-12.

(5) Lazar, M.; Varghese, S.; Nair, S. Photocatalytic Water Treatment By Titanium Dioxide: Recent Updates. *Catalysts* **2012**, 2, 572-601.

(6) Li, Y.; Xie, W.; Hu, X.; Shen, G.; Zhou, X.; Xiang, Y.; Zhao, X.; Fang, P. Comparison Of Dye Photodegradation And Its Coupling With Light-To-Electricity Conversion Over TiO_2 And ZnO. *Langmuir* **2009**, *26*, 591-597.

(7) Luo, L.; Cooper, A.; Fan, M. Preparation And Application Of Nanoglued Binary Titania–Silica Aerogel. *Journal of Hazardous Materials* **2009**, *161*, 175-182.

(8) He, Y.; Zhang, L.; Wang, X.; Wu, Y.; Lin, H.; Zhao, L.; Weng, W.; Wan, H.; Fan, M. Enhanced Photodegradation Activity Of Methyl Orange Over Z-Scheme Type MoO_3-g-C_3N_4 Composite Under Visible Light Irradiation. *RSC Adv.* **2014**, *4*, 13610-13619.

(9) Rajeshwar, K.; Osugi, M.; Chanmanee, W.; Chenthamarakshan, C.; Zanoni, M.; Kajitvichyanukul, P.; Krishnan-Ayer, R. Heterogeneous Photocatalytic Treatment Of Organic Dyes In Air And Aqueous Media. *Journal of Photochemistry and Photobiology C: Photochemistry Reviews* **2008**, *9*, 171-192.

(10) Drumond Chequer, F.; de Oliveira, G.; Anastacio Ferraz, E.; Carvalho, J.; Boldrin Zanoni, M.; de Oliveir, D. Textile Dyes: Dyeing Process And Environmental Impact. *Eco-Friendly Textile Dyeing and Finishing* **2013**.

(11) Forgacs, E.; Cserháti, T.; Oros, G. Removal Of Synthetic Dyes From Wastewaters: A Review. *Environment International* **2004**, 30, 953-971.

(12) Galindo, C.; Jacques, P.; Kalt, A. Photooxidation Of The Phenylazonaphthol AO20 On TIO2: Kinetic And Mechanistic Investigations. *Chemosphere* **2001**, 45, 997-1005.

(13) Priyaragini, S.; Veena, S.; Swetha, D.; Karthik, L.; Kumar, G.; Bhaskara Rao, K. Evaluating The Effectiveness Of Marine Actinobacterial Extract And Its Mediated Titanium Dioxide Nanoparticles In The Degradation Of Azo Dyes. *Journal of Environmental Sciences* **2014**, 26, 775-782.

(14) Pan, H.; Feng, J.; He, G.; Cerniglia, C.; Chen, H. Evaluation Of Impact Of Exposure Of Sudan Azo Dyes And Their Metabolites On Human Intestinal Bacteria. *Anaerobe* **2012**, 18, 445-453.

(15) Jo, W.; Tayade, R. Recent Developments In Photocatalytic Dye Degradation Upon Irradiation With Energy-Efficient Light Emitting Diodes. *Chinese Journal of Catalysis* **2014**, *35*, 1781-1792.
(16) Muhd Julkapli, N.; Bagheri, S.; Bee Abd Hamid, S. Recent Advances In Heterogeneous Photocatalytic Decolorization Of Synthetic Dyes. *The Scientific World Journal* **2014**, *2014*, 1-25.
(17) Qu, J.; Fan, M. The Current State Of Water Quality And Technology Development For Water Pollution Control In China. *Critical Reviews in Environmental Science and Technology* **2010**, 40, 519-560.
(18) Mahmoodi, N.; Arami, M. Degradation And Toxicity Reduction Of Textile Wastewater Using Immobilized Titania Nanophotocatalysis. *Journal of Photochemistry and Photobiology B: Biology* **2009**, *94*, 20-24.
(19) Akyol, A.; Yatmaz, H.; Bayramoglu, M. Photocatalytic Decolorization Of Remazol Red RR In Aqueous Zno Suspensions. *Applied Catalysis B: Environmental* **2004**, *54*, 19-24.
(20) Baldrian, P.; Merhautová, V.; Gabriel, J.; Nerud, F.; Stopka, P.; Hrubý, M.; Beneš, M. Decolorization Of Synthetic Dyes By Hydrogen Peroxide With Heterogeneous Catalysis By Mixed Iron Oxides. *Applied Catalysis B: Environmental* **2006**, *66*, 258-264.
(21) Spagni, A.; Grilli, S.; Casu, S.; Mattioli, D. Treatment Of A Simulated Textile Wastewater Containing The Azo-Dye Reactive Orange 16 In An Anaerobic-Biofilm Anoxic–Aerobic Membrane Bioreactor. *International Biodeterioration & Biodegradation* **2010**, *64*, 676-681.
(22) Koprivanac, N.; Kusic, H. *Hazardous Organic Pollutants In Colored Wastewaters*; Nova Science Publishers: New York, **2009**.
(23) Ganzenko, O.; Huguenot, D.; van Hullebusch, E.; Esposito, G.; Oturan, M. Electrochemical Advanced Oxidation And Biological Processes For Wastewater Treatment: A Review Of The Combined Approaches. *Environmental Science and Pollution Research* **2014**, 21, 8493-8524.
(24) Ray, S.; Takafuji, M.; Ihara, H. Peptide-Based Surface Modified Silica Particles: Adsorption Materials For Dye-Loaded Wastewater Treatment. *RSC Advances* **2013**, 3, 23664.
(25) Rao, A.; Sivasankar, B.; Sadasivam, V. Kinetic Studies On The Photocatalytic Degradation Of Direct Yellow 12 In The Presence Of Zno Catalyst. *Journal of Molecular Catalysis A: Chemical* **2009**, 306, 77-81.
(26) Sobana, N.; Swaminathan, M. Combination Effect Of Zno And Activated Carbon For Solar Assisted Photocatalytic Degradation Of Direct Blue 53. *Solar Energy Materials and Solar Cells* **2007**, 91, 727-734.
(27) Anwer, H.; Mahmood, A.; Lee, J.; Kim, K.; Park, J.; Yip, A. Photocatalysts For Degradation Of Dyes In Industrial Effluents: Opportunities And Challenges. *Nano Research* **2019**, *12*, 955-972.
(28) Azbar, N.; Yonar, T.; Kestioglu, K. Comparison Of Various Advanced Oxidation Processes And Chemical Treatment Methods For COD And Color Removal From A Polyester And Acetate Fiber Dyeing Effluent. *Chemosphere* **2004**, 55, 35-43.
(29) Chen, D.; Sivakumar, M.; Ray, A. Heterogeneous Photocatalysis In Environmental Remediation. *Developments in Chemical Engineering and Mineral Processing* **2008**, *8*, 505-550.
(30) Li, C.; Wei, M.; Evans, D.; Duan, X. Layered Double Hydroxide-Based Nanomaterials As Highly Efficient Catalysts And Adsorbents. *Small* **2014**, *10*, 4469-4486.
(31) Kudo, A.; Miseki, Y. Heterogeneous Photocatalyst Materials For Water Splitting. *Chem. Soc. Rev.* **2009**, *38*, 253-278.
(32) Xiang, Q.; Yu, J.; Jaroniec, M. Graphene-Based Semiconductor Photocatalysts. *Chem. Soc. Rev.* **2012**, *41*, 782-796.

(33) Chatterjee, D.; Dasgupta, S. Visible Light Induced Photocatalytic Degradation Of Organic Pollutants. *Journal of Photochemistry and Photobiology C: Photochemistry Reviews* **2005**, *6*, 186-205.
(34) Ohtani, B. Photocatalysis A To Z—What We Know And What We Do Not Know In A Scientific Sense. *Journal of Photochemistry and Photobiology C: Photochemistry Reviews* **2010**, 11, 157-178.
(35) Tahir, M.; Rafique, M.; Rafique, M.; Fatima, N.; Israr, Z. Metal Oxide- And Metal Sulfide-Based Nanomaterials As Photocatalysts. *Nanotechnology and Photocatalysis for Environmental Applications* **2020**, 77-96.
(36) Cho, B.; Ko, W. Preparation Of Graphene-ZrO_2 Nanocomposites By Heat Treatment And Photocatalytic Degradation Of Organic Dyes. *Journal of Nanoscience and Nanotechnology* **2013**, 13 (11), 7625-7630.
(37) Dong, S.; Feng, J.; Fan, M.; Pi, Y.; Hu, L.; Han, X.; Liu, M.; Sun, J.; Sun, J. Recent Developments In Heterogeneous Photocatalytic Water Treatment Using Visible Light-Responsive Photocatalysts: A Review. *RSC Advances* **2015**, *5*, 14610-14630.
(38) Mori, K.; Yamashita, H. Progress In Design And Architecture Of Metal Nanoparticles For Catalytic Applications. *Physical Chemistry Chemical Physics* **2010**, 12, 14420.
(39) Qu, X.; Alvarez, P.; Li, Q. Applications Of Nanotechnology In Water And Wastewater Treatment. *Water Research* **2013**, 47, 3931-3946.
(40) Yan, X.; Xu, L.; Huang, W.; Huang, G.; Yang, Z.; Zhan, S.; Long, J. Theoretical Insight Into The Electronic And Photocatalytic Properties Of Cu_2O From A Hybrid Density Functional Theory. *Materials Science in Semiconductor Processing* **2014**, 23, 34-41.
(41) Zhu, X.; Zhang, J.; Chen, F. Hydrothermal Synthesis Of Nanostructures Bi12tio20 And Their Photocatalytic Activity On Acid Orange 7 Under Visible Light. *Chemosphere* **2010**, 78, 1350-1355.
(42) Imtiaz, F.; Rashid, J.; Xu, M. Semiconductor Nanocomposites For Visible Light Photocatalysis Of Water Pollutants. *Concepts of Semiconductor Photocatalysis* **2019**.
(43) Wang, Y.; Wang, X.; Antonietti, M. Polymeric Graphitic Carbon Nitride As A Heterogeneous Organocatalyst: From Photochemistry To Multipurpose Catalysis To Sustainable Chemistry. *Angewandte Chemie International Edition* **2011**, *51*, 68-89.
(44) Xu, Y.; Gao, S. Band Gap Of C3N4 In The GW Approximation. *International Journal of Hydrogen Energy* **2012**, *37*, 11072-11080.
(45) Siavash Moakhar, R.; Hosseini‐Hosseinabad, S.; Masudy‐Panah, S.; Seza, A.; Jalali, M.; Fallah‐Arani, H.; Dabir, F.; Gholipour, S.; Abdi, Y.; Bagheri‐Hariri, M.; Riahi‐Noori, N.; Lim, Y.; Hagfeldt, A.; Saliba, M. Photoelectrochemical Water‐Splitting Using Cuo‐Based Electrodes For Hydrogen Production: A Review. *Advanced Materials* **2021**, *33*, 2007285.
(46) Chen, C.; Ma, W.; Zhao, J. Semiconductor-Mediated Photodegradation Of Pollutants Under Visible-Light Irradiation. *Chemical Society Reviews* **2010**, *39*, 4206.
(47) Watanabe, T.; Takizawa, T.; Honda, K. Photocatalysis Through Excitation Of Adsorbates. 1. Highly Efficient N-Deethylation Of Rhodamine B Adsorbed To Cadmium Sulfide. *The Journal of Physical Chemistry* 1977, *81*, 1845-1851.
(48) Vinodgopal, K.; Wynkoop, D.; Kamat, P. Environmental Photochemistry On Semiconductor Surfaces: Photosensitized Degradation Of A Textile Azo Dye, Acid Orange 7, On Tio2 Particles Using Visible Light. Environmental Science & Technology 1996, 30, 1660-1666.
(49) Hisatomi, T.; Domen, K. Reaction Systems For Solar Hydrogen Production Via Water Splitting With Particulate Semiconductor Photocatalysts. *Nature Catalysis* **2019**, *2*, 387-399.

(50) Ning, F.; Shao, M.; Xu, S.; Fu, Y.; Zhang, R.; Wei, M.; Evans, D.; Duan, X. Tio2/Graphene/Nife-Layered Double Hydroxide Nanorod Array Photoanodes For Efficient Photoelectrochemical Water Splitting. *Energy & Environmental Science* **2016**, *9*, 2633-2643.
(51) Wadsworth, A.; Moser, M.; Marks, A.; Little, M.; Gasparini, N.; Brabec, C.; Baran, D.; McCulloch, I. Critical Review Of The Molecular Design Progress In Non-Fullerene Electron Acceptors Towards Commercially Viable Organic Solar Cells. *Chemical Society Reviews* **2019**, *48*, 1596-1625.
(52) Hisatomi, T.; Kubota, J.; Domen, K. Recent Advances In Semiconductors For Photocatalytic And Photoelectrochemical Water Splitting. *Chem. Soc. Rev.* 2014, *43*, 7520-7535.
(53) Kudo, A.; Miseki, Y. Heterogeneous Photocatalyst Materials For Water Splitting. *Chem. Soc. Rev.* **2009**, *38*, 253-278.
(54) Yang, W.; Prabhakar, R.; Tan, J.; Tilley, S.; Moon, J. Strategies For Enhancing The Photocurrent, Photovoltage, And Stability Of Photoelectrodes For Photoelectrochemical Water Splitting. *Chemical Society Reviews* **2019**, *48*, 4979-5015.
(55) Azevedo, J.; Tilley, S.; Schreier, M.; Stefik, M.; Sousa, C.; Araújo, J.; Mendes, A.; Grätzel, M.; Mayer, M. Tin Oxide As Stable Protective Layer For Composite Cuprous Oxide Water-Splitting Photocathodes. *Nano Energy* **2016**, *24*, 10-16.
(56) Nishikawa, M.; Fukuda, M.; Nakabayashi, Y.; Saito, N.; Ogawa, N.; Nakajima, T.; Shinoda, K.; Tsuchiya, T.; Nosaka, Y. A Method To Give Chemically Stabilities Of Photoelectrodes For Water Splitting: Compositing Of A Highly Crystalized Tio2 Layer On A Chemically Unstable Cu2o Photocathode Using Laser-Induced Crystallization Process. *Applied Surface Science* **2016**, *363*, 173-180.
(57) Konstantinou, I.; Albanis, T. Tio2-Assisted Photocatalytic Degradation Of Azo Dyes In Aqueous Solution: Kinetic And Mechanistic Investigations. *Applied Catalysis B: Environmental* **2004**, 49.
(58) Chakrabarti, S.; Dutta, B. Photocatalytic Degradation Of Model Textile Dyes In Wastewater Using Zno As Semiconductor Catalyst. *Journal of Hazardous Materials* **2004**, 112, 269-278.
(59) Reddy, M.; Venugopal, A.; Subrahmanyam, M. Hydroxyapatite Photocatalytic Degradation Of Calmagite (An Azo Dye) In Aqueous Suspension. *Applied Catalysis B: Environmental* **2007**, 69, 164-170.
(60) Akpan, U.; Hameed, B. Parameters Affecting The Photocatalytic Degradation Of Dyes Using Tio2-Based Photocatalysts: A Review. *Journal of Hazardous Materials* **2009**, 170, 520-529.
(61) Jung, J.; Jang, J.; Park, J. Effect Of Generation Growth On Photocatalytic Activity Of Nano TiO_2-Magnetic Cored Dendrimers. *Journal of Industrial and Engineering Chemistry* **2016**, 44, 52-59.
(62) Zangeneh, H.; Zinatizadeh, A.; Habibi, M.; Akia, M.; Hasnain Isa, M. Photocatalytic Oxidation Of Organic Dyes And Pollutants In Wastewater Using Different Modified Titanium Dioxides: A Comparative Review. *Journal of Industrial and Engineering Chemistry* **2015**, 26, 1-36.
(63) Sibhatu, A.; Weldegebrieal, G.; Sagadevan, S.; Tran, N.; Hessel, V. Photocatalytic Activity Of Cuo Nanoparticles For Organic And Inorganic Pollutants Removal In Wastewater Remediation. *Chemosphere* **2022**, *300*, 134623.
(64) Lü, W.; Chen, J.; Wu, Y.; Duan, L.; Yang, Y.; Ge, X. Graphene-Enhanced Visible-Light Photocatalysis Of Large-Sized Cds Particles For Wastewater Treatment. *Nanoscale Research Letters* **2014**, 9.
(65) Anwer, H.; Park, J. Synthesis And Characterization Of A Heterojunction $rGO/ZrO_2/Ag_3PO_4$ Nanocomposite For Degradation Of Organic Contaminants. *Journal of Hazardous Materials* **2018**, 358, 416-426.

(66) Zhang, A.; Wang, W.; Pei, D.; Yu, H. Degradation Of Refractory Pollutants Under Solar Light Irradiation By A Robust And Self-Protected Zno/Cds/Tio2 Hybrid Photocatalyst. *Water Research* **2016**, 92, 78-86.
(67) Li, X.; Wang, J.; Men, Y.; Bian, Z. Tio 2 Mesocrystal With Exposed (001) Facets And Cds Quantum Dots As An Active Visible Photocatalyst For Selective Oxidation Reactions. *Applied Catalysis B: Environmental* **2016**, 187, 115-121.
(68) Bhandari, S.; Vardia, J.; Malkani, R.; Ameta, S. Effect Of Transition Metal Ions On Photocatalytic Activity Of Zno In Bleaching Of Some Dyes. *Toxicological & Environmental Chemistry* **2006**, 88, 35-44.
(69) Ajmal, A.; Majeed, I.; Malik, R.; Idriss, H.; Nadeem, M. Principles And Mechanisms Of Photocatalytic Dye Degradation On TiO_2 Based Photocatalysts: A Comparative Overview. *RSC Adv.* **2014**, 4, 37003-37026.
(70) Schneider, S. UV/VIS-Spektroskopie Für Analytiker: UV-VIS Spectroscopy And Its Applications. Von H. -H. Perkampus. Springer, Heidelberg, 1992. 244 S., 78 Abb., 21 Tab., Geb. DM 168,-. ISBN 3-540-55421-1. *Nachrichten aus Chemie, Technik und Laboratorium* **1993**, 41, 1274-1277.
(71) Nguyen-Phan, T.; Pham, V.; Shin, E.; Pham, H.; Kim, S.; Chung, J.; Kim, E.; Hur, S. The Role Of Graphene Oxide Content On The Adsorption-Enhanced Photocatalysis Of Titanium Dioxide/Graphene Oxide Composites. *Chemical Engineering Journal* **2011**, 170, 226-232.
(72) Bizani, E.; Fytianos, K.; Poulios, I.; Tsiridis, V. Photocatalytic Decolorization And Degradation Of Dye Solutions And Wastewaters In The Presence Of Titanium Dioxide. *Journal of Hazardous Materials* **2006**, 136, 85-94.
(73) Tan, R.; Shen, Y.; Roberts, S. K.; Gee, M. Y.; Blom, D. A.; Greytak, A. B. Reducing competition by coordinating solvent promotes morphological control in alternating layer growth of CdSe/CdS core/shell quantum dots. *Chem. Mater.* **2015**, 27, 7468–7480.
(74) Xu, Z.; Liu, X. X.; Wang, W. P.; Liu, C.; Li, Z. C.; Zhang, Z. J. Enhanced photoelectrochemical properties of TiO2 nanorod arrays decorated with CdS nanoparticles. *Sci. Technol. Adv. Mater.* **2014**, 15, 055006.
(75) Cassano, A. E.; Alfano, O. M. Reaction engineering of suspended solid heterogeneous photocatalytic reactors. *Catal. Today* **2000**, 58, 167–197.
(76) Muruganandham, M.; Swaminathan, M. TiO2–UV photocatalytic oxidation of Reactive Yellow 14: Effect of operational parameters. *J. Hazard. Mater.* **2006**, 135, 78–86.
(77) Bhati, I.; Punjabi, P. B.; Ameta, S. C. Photocatalytic degradation of fast green using nanosized CeCrO3. *Maced. J. Chem. Chem. Eng*. **2010**, 29, 195–202.
(78) Elaziouti; Laouedj, N.; Ahmed, B. ZnO-assisted photocatalytic degradation of Congo Red and Benzopurpurine 4B in aqueous solution. *J. Chem. Eng. Process Technol.* **2011**, 2, 106.
(79) Evgenidou, E.; Fytianos, K.; Poulios, I. Semiconductor-Sensitized Photodegradation Of Dichlorvos In Water Using Tio2 And Zno As Catalysts. *Applied Catalysis B: Environmental* **2005**, *59*, 81-89.
(80) Canle L., M.; Santaballa, J.; Vulliet, E. On The Mechanism Of Tio2-Photocatalyzed Degradation Of Aniline Derivatives. *Journal of Photochemistry and Photobiology A: Chemistry* **2005**, *175*, 192-200.
(81) Lhomme, L.; Brosillon, S.; Wolbert, D.; Dussaud, J. Photocatalytic Degradation Of A Phenylurea, Chlortoluron, In Water Using An Industrial Titanium Dioxide Coated Media. *Applied Catalysis B: Environmental* **2005**, *61*, 227-235.
(82) Chatterjee, D.; Dasgupta, S. Visible Light Induced Photocatalytic Degradation Of Organic Pollutants. *Journal of Photochemistry and Photobiology C: Photochemistry Reviews* **2005**, *6*, 186-205.

(83) Rauf, M.; Ashraf, S. Fundamental Principles And Application Of Heterogeneous Photocatalytic Degradation Of Dyes In Solution. *Chemical Engineering Journal* **2009**, *151*, 10-18.
(84) Neppolian, B.; Choi, H.; Sakthivel, S.; Arabindoo, B.; Murugesan, V. Solar Light Induced And TiO_2 Assisted Degradation Of Textile Dye Reactive Blue 4. *Chemosphere* **2002**, *46*, 1173-1181.
(85) Shukla, K.; Srivastava, V. C. Diethyl carbonate: Critical review of synthesis routes, catalysts used and engineering aspects. *RSC Adv.* **2016**, 6, 32624–32645.
(86) He, Z.; Lin, L.; Song, S.; Xia, M.; Xu, L.; Ying, H.; Chen, J. Mineralization Of C.I. Reactive Blue 19 By Ozonation Combined With Sonolysis: Performance Optimization And Degradation Mechanism. *Separation and Purification Technology* **2008**, *62*, 376-381.
(87) Han, Y.; Phonthammachai, N.; Ramesh, K.; Zhong, Z.; White, T. Removing Organic Compounds From Aqueous Medium Via Wet Peroxidation By Gold Catalysts. *Environmental Science & Technology* **2007**, *42*, 908-912.
(88) Zhang, F.; Yediler, A.; Liang, X.; Kettrup, A. Effects Of Dye Additives On The Ozonation Process And Oxidation By-Products: A Comparative Study Using Hydrolyzed C.I. Reactive Red 120. *Dyes and Pigments* **2004**, *60*, 1-7.
(89) Ashraf, S.; Rauf, M.; Alhadrami, S. Degradation Of Methyl Red Using Fenton's Reagent And The Effect Of Various Salts. *Dyes and Pigments* **2006**, *69*, 74-78.
(90) Muruganandham, M. Photochemical Oxidation Of Reactive Azo Dye With UV–H2O2 Process. *Dyes and Pigments* **2004**, *62*, 269-275.
(91) Yoon, J.; Lee, Y.; Kim, S. Investigation Of The Reaction Pathway Of OH Radicals Produced By Fenton Oxidation In The Conditions Of Wastewater Treatment. *Water Science and Technology* **2001**, *44*, 15-15.
(92) Alnuaimi, M.; Rauf, M.; Ashraf, S. A Comparative Study Of Neutral Red Decoloration By Photo-Fenton And Photocatalytic Processes. *Dyes and Pigments* **2008**, *76*, 332-337.
(93) Xu, X.; Li, H.; Gu, J. Simultaneous Decontamination Of Hexavalent Chromium And Methyl Tert-Butyl Ether By UV/Tio2 Process. *Chemosphere* **2006**, *63*, 254-260.
(94) Tayade, R.; Surolia, P.; Kulkarni, R.; Jasra, R. Photocatalytic Degradation Of Dyes And Organic Contaminants In Water Using Nanocrystalline Anatase And Rutile Tio2. *Science and Technology of Advanced Materials* **2007**, *8*, 455-462.
(95) Mills, A.; Lee, S.; Lepre, A.; Parkin, I.; O'Neill, S. Spectral And Photocatalytic Characteristics Of Tio2 CVD Films On Quartz. *Photochemical & Photobiological Sciences* **2002**, *1*, 865-868.
(96) Nanocomposites For Visible Light-Induced Photocatalysis. *Springer Series on Polymer and Composite Materials* **2017**.
(97) Fujishima, A.; Honda, K. Electrochemical photolysis of water at a semiconductor electrode. *Nature* **1972**, 238, 37–38.
(98) Teets, T.; Nocera, D. Photocatalytic Hydrogen Production. *Chemical Communications* **2011**, *47*, 9268.
(101) Meyer, B.; Polity, A.; Reppin, D.; Becker, M.; Hering, P.; Klar, P.; Sander, T.; Reindl, C.; Benz, J.; Eickhoff, M.; Heiliger, C.; Heinemann, M.; Bläsing, J.; Krost, A.; Shokovets, S.; Müller, C.; Ronning, C. Binary Copper Oxide Semiconductors: From Materials Towards Devices. *physica status solidi (b)* **2012**, *249*, 1487-1509.
(102) Zhang, X.; Zhang, D.; Ni, X.; Song, J.; Zheng, H. Synthesis And Electrochemical Properties Of Different Sizes Of The Cuo Particles. *Journal of Nanoparticle Research* **2007**, *10*, 839-844.

(103) Volanti, D.; Keyson, D.; Cavalcante, L.; Simões, A.; Joya, M.; Longo, E.; Varela, J.; Pizani, P.; Souza, A. Synthesis And Characterization Of Cuo Flower-Nanostructure Processing By A Domestic Hydrothermal Microwave. *Journal of Alloys and Compounds* **2008**, *459*, 537-542.
(104) Eliseev, A.; Lukashin, A.; Vertegel, A.; Heifets, L.; Zhirov, A.; Tretyakov, Y. Complexes Of Cu(II) With Polyvinyl Alcohol As Precursors For The Preparation Of Cuo/Sio2nanocomposites. *Materials Research Innovations* **2000**, *3*, 308-312.
(105) Vidyasagar, C.; Arthoba Naik, Y.; Venkatesha, T.; Viswanatha, R. Solid-State Synthesis And Effect Of Temperature On Optical Properties Of Cuo Nanoparticles. *Nano-Micro Letters* **2012**, *4*, 73-77.
(106) Karthikeyan, C.; Karuppuchamy, S. Synthesis Of Novel Cuo–Al2o3 Catalyst For Biodiesel Production. *Advanced Science, Engineering and Medicine* **2017**, *9*, 1011-1016.
(107) Kumar, R.; Diamant, Y.; Gedanken, A. Sonochemical Synthesis And Characterization Of Nanometer-Size Transition Metal Oxides From Metal Acetates. *Chemistry of Materials* **2000**, *12*, 2301-2305.
(108) Li, Y.; Kuai, P.; Huo, P.; Liu, C. Fabrication Of Cuo Nanofibers Via The Plasma Decomposition Of Cu(OH)2. *Materials Letters* **2009**, *63*, 188-190.
(109) Zoolfakar, A.; Rani, R.; Morfa, A.; O'Mullane, A.; Kalantar-zadeh, K. Nanostructured Copper Oxide Semiconductors: A Perspective On Materials, Synthesis Methods And Applications. *J. Mater. Chem. C* **2014**, 2 (27), 5247-5270.
(110) Dung, N.; Le, D.; Trung, N.; Dung, H.; Hung, N.; Duy, N.; Hoa, N.; Hieu, N. Cuo Nanofibers Prepared By Electrospinning For Gas Sensing Application: Effect Of Copper Salt Concentration. *Journal of Nanoscience and Nanotechnology* **2016**, 16 (8), 7910-7918.

(111) Fan, J.; Tang, D.; Wang, D. Spontaneous Growth Of Cuo Nanoflakes And Microflowers On Copper In Alkaline Solutions. *Journal of Alloys and Compounds* **2017**, 704, 624-630.

(112) Keabadile, O.; Aremu, A.; Elugoke, S.; Fayemi, O. Green And Traditional Synthesis Of Copper Oxide Nanoparticles—Comparative Study. *Nanomaterials* **2020**, 10 (12), 2502.

(113) Yang, L.; Chu, D.; Wang, L. Porous Hexapod Cuo Nanostructures: Precursor-Mediated Fabrication, Characterization, And Visible-Light Induced Photocatalytic Degradation Of Phenol. *Materials Letters* **2015**, 160, 246-249.

(114) Natarajan, S.; Bajaj, H.; Tayade, R. Recent advances based on the synergetic effect of adsorption for removal of dyes from waste water using photocatalytic process. *Journal of environmental sciences* **2018**, 65, 201-222.

(115) Nguyen, D.; Cho, K.; Oh, W. Synthesis Of Frost-Like Cuo Combined Graphene-Tio 2 By Self-Assembly Method And Its High Photocatalytic Performance. *Applied Surface Science* **2017**, *412*, 252-261.

(116) Masudy-Panah, S.; Radhakrishnan, K.; Tan, H.; Yi, R.; Wong, T.; Dalapati, G. Titanium Doped Cupric Oxide For Photovoltaic Application. *Solar Energy Materials and Solar Cells* **2015**, *140*, 266-274.

(117) Vo, T.; Chang, S.; Chiang, C. Anion-Induced Morphological Regulation Of Cupric Oxide Nanostructures And Their Application As Co-Catalysts For Solar Water Splitting. *Dalton Transactions* **2020**, *49*, 1765-1775.

(118) Masudy-Panah, S.; Siavash Moakhar, R.; Chua, C.; Tan, H.; Wong, T.; Chi, D.; Dalapati, G. Nanocrystal Engineering Of Sputter-Grown Cuo Photocathode For Visible-Light-Driven Electrochemical Water Splitting. *ACS Applied Materials & Interfaces* **2016**, *8*, 1206-1213.

(119) Zaleska-Medynska, A. *Metal Oxide-Based Photocatalysis*; Elsevier: Amsterdam, **2018**.

(120) Gu, Y.; Xuan, Y.; Zhang, H.; Deng, X.; Bai, M.; Wang, L. A facile coordination precipitation route to prepare porous CuO microspheres with excellent photo-Fenton catalytic activity and electrochemical performance. *CrystEngComm* **2019**, 21, 648–655.

(121) Wang, X.; Yang, J.; Shi, L.; Gao, M. Surfactant-free synthesis of CuO with controllable morphologies and enhanced photocatalytic property. *Nanoscale Res. Lett.* **2016**, 11, 125.

(122) Zeng, Q.; Xu, G.; Zhang, L.; Lin, H.; Lv, Y.; Jia, D. Porous CuO nanofibers derived from a Cu-based coordination polymer as a photocatalyst for the degradation of rhodamine B. *New J. Chem.* **2018**, 42, 7016–7024.

(123) Li, J.; Sun, F.; Gu, K.; Wu, T.; Zhai, W.; Li, W.; Huang, S. Preparation Of Spindly Cuo Micro-Particles For Photodegradation Of Dye Pollutants Under A Halogen Tungsten Lamp. *Applied Catalysis A: General* **2011**, 406 (1-2), 51-58.

(124) Yang, C.; Wang, J.; Xiao, F.; Su, X. Microwave Hydrothermal Disassembly For Evolution From Cuo Dendrites To Nanosheets And Their Applications In Catalysis And Photo-Catalysis. *Powder Technology* **2014**, 264, 36-42.

(125) Liu, Q.; Sun, J.; Han, D.; Liu, X.; Gao, X.; Jiang, Y.; Xie, K. Highly Efficient Photocatalytic Removal Of Methylene Blue By Lamellar Structured Nanocrystalline And Amorphous Cuo. *Materials Letters* **2020**, 276, 128217.

(126) Sorekine, G.; Anduwan, G.; Waimbo, M.; Osora, H.; Velusamy, S.; Kim, S.; Kim, Y.; Charles, J. Photocatalytic Studies Of Copper Oxide Nanostructures For The Degradation Of Methylene Blue Under Visible Light. *Journal of Molecular Structure* **2022**, 1248, 131487.

(127) Liu, Q.; Deng, W.; Wang, Q.; Lin, X.; Gong, L.; Liu, C.; Xiong, W.; Nie, X. An Efficient Chemical Precipitation Route To Fabricate 3D Flower-Like Cuo And 2D Leaf-Like Cuo For Degradation Of Methylene Blue. *Advanced Powder Technology* **2020**, 31 (4), 1391-1401.

(128) Lobna, A.; Janene, F.; Kouass, S.; Mignard, S.; Touati, F.; Dhaouadi, H. Cuo Nanosheets: Synthesis, Characterization, And Catalytic Performance. *Russian Journal of Inorganic Chemistry* **2019**, 64 (13), 1687-1696.

(129) Lakhotiya, G.; Bajaj, S.; Nayak, A.; Pradhan, D.; Tekade, P.; Rana, A. Enhanced Catalytic Activity Without The Use Of An External Light Source Using Microwave-Synthesized Cuo Nanopetals. *Beilstein Journal of Nanotechnology* **2017**, 8, 1167-1173.

(130) Hu, J.; Chen, M.; Fang, X.; Wu, L. Fabrication And Application Of Inorganic Hollow Spheres. *Chemical Society Reviews* **2011**, 40 (11), 5472.

(131) Wang, X.; Feng, J.; Bai, Y.; Zhang, Q.; Yin, Y. Synthesis, Properties, And Applications Of Hollow Micro-/Nanostructures. *Chemical Reviews* **2016**, 116 (18), 10983-11060.

(132) Rabbani, M.; Rahimi, R.; Bozorgpour, M.; Shokraiyan, J.; Moghaddam, S. Photocatalytic Application Of Hollow Cuo Microspheres With Hierarchical Dandelion-Like Structures Synthesized By A Simple Template Free Approach. *Materials Letters* **2014**, 119, 39-42.

(133) Reza, K.; Kurny, A.; Gulshan, F. Parameters Affecting The Photocatalytic Degradation Of Dyes Using Tio2: A Review. *Applied Water Science* **2015**, *7*, 1569-1578.